

# 1 Lability classification of soil organic matter in the northern permafrost region

2  
3 *Kuhry, P.<sup>1</sup>, Bárta, J.<sup>2</sup>, Blok, D.<sup>3</sup>, Elberling, B.<sup>4</sup>, Faucherre, S.<sup>4</sup>, Hugelius, G.<sup>1,5</sup>, Jørgensen, C. J.<sup>4,6</sup>,*  
4 *Richter, A.<sup>7</sup>, Šantrůčková, H.<sup>2</sup> and Weiss, N.<sup>1,8</sup>*

5  
6 <sup>1)</sup> *Department of Physical Geography, Stockholm University, Sweden*

7 <sup>2)</sup> *Department of Ecosystem Biology, University of South Bohemia, Ceske Budejovice, Czech Republic*

8 <sup>3)</sup> *Department of Physical Geography and Ecosystem Science, Lund University, Sweden*

9 <sup>4)</sup> *Center for Permafrost (CENPERM), Department of Geosciences and Natural Resource Management, University of*  
10 *Copenhagen, Denmark*

11 <sup>5)</sup> *Bolin Centre for Climate Research, Stockholm University, Sweden*

12 <sup>6)</sup> *Current affiliation: Department of Bioscience, Section for Arctic Environment, Aarhus University, Denmark*

13 <sup>7)</sup> *Department of Microbiology and Ecosystem Science, University of Vienna, Austria*

14 <sup>8)</sup> *Current affiliation: Department of Geography and Environmental Studies, Wilfrid Laurier University, Yellowknife,*  
15 *Canada*

16  
17 Correspondence email: [peter.kuhry@natgeo.su.se](mailto:peter.kuhry@natgeo.su.se)

## 18 19 Abstract

20  
21 The large stocks of soil organic carbon (SOC) in soils and deposits of the northern permafrost region  
22 are sensitive to global warming and permafrost thawing. The potential release of this carbon (C) as  
23 greenhouse gases to the atmosphere does not only depend on the total quantity of soil organic matter  
24 (SOM) affected by warming and thawing, but also on its lability (i.e. the rate at which it will decay).  
25 In this study we develop a simple and robust classification scheme of SOM lability for the main  
26 types of soils and deposits in the northern permafrost region. The classification is based on widely  
27 available soil geochemical parameters and landscape unit classes, which makes it useful for  
28 upscaling to the entire northern permafrost region. We have analyzed the relationship between C  
29 content and C-CO<sub>2</sub> production rates of soil samples in two different types of laboratory incubation  
30 experiment. In one experiment, c. 240 soil samples from four study areas were incubated using the  
31 same protocol (at 5 °C, aerobically) over a period of one year. Here we present C release rates  
32 measured on day 343 of incubation. These long-term results are compared to those obtained from  
33 short-term incubations of c. 1000 samples (at 12 °C, aerobically) from an additional three study  
34 areas. In these experiments, C-CO<sub>2</sub> production rates were measured over the first four days of  
35 incubation. We have focused our analyses on the relationship between C-CO<sub>2</sub> production per gram  
36 dry weight per day ( $\mu\text{gC-CO}_2 \text{gdw}^{-1} \text{d}^{-1}$ ) and C content (%C of dry weight) in the samples, but show  
37 that relationships are consistent when using C/N ratios or different production units such as  $\mu\text{gC}$  per  
38 gram soil C per day ( $\mu\text{gC-CO}_2 \text{gC}^{-1} \text{d}^{-1}$ ) or per cm<sup>3</sup> of soil per day ( $\mu\text{gC-CO}_2 \text{cm}^{-3} \text{d}^{-1}$ ). C content of  
39 the samples is positively correlated to C-CO<sub>2</sub> production rates but explains less than 50 % of the  
40 observed variability when the full datasets are considered. A partitioning of the data into landscape  
41 units greatly reduces variance and provides consistent results between incubation experiments. These  
42 results indicate that relative SOM lability decreases in the order: Late Holocene eolian deposits >  
43 alluvial deposits and mineral soils (including peaty wetlands) > Pleistocene Yedoma deposits > C-  
44 enriched pockets in cryoturbated soils > peat deposits. Thus, three of the most important SOC  
45 storage classes in the northern permafrost region (Yedoma, cryoturbated soils and peatlands) show  
46 low relative SOM lability. Previous research has suggested that SOM in these pools is relatively  
47 undecomposed and the reasons for the observed low rates of decomposition in our experiments need

48 urgent attention if we want to better constrain the magnitude of the thawing permafrost carbon  
49 feedback on global warming.

50

## 51 1. Introduction

52

53 Permafrost has been recognized as one of the vulnerable carbon (C) pools in the Earth System  
54 (Gruber et al., 2004). A recent report of the International Panel on Climate Change (IPCC, 2018)  
55 identifies the thawing permafrost carbon-climate feedback as one of the key uncertainties when  
56 assessing global emission targets to keep global warming under 1.5 (2) °C. Furthermore, the urgency  
57 of additional research is highlighted by the fact that most permafrost in the northern circumpolar  
58 region has already experienced warming in recent decades (Biskaborn et al., 2019).

59 In the last decade there has been a surge in papers dealing with the permafrost carbon feedback  
60 on climate change (e.g. Schuur et al., 2008; Kuhry et al., 2010). This increased interest was fueled by  
61 a new and high estimate of the total soil organic carbon (SOC) storage in the northern permafrost  
62 region (Tarnocai et al., 2009), which was received with great interest by the Earth System Science  
63 community (e.g., Ciais, 2009). Since this first new estimate was published, a multitude of new SOC  
64 inventories at the landscape level have been conducted across the Circumpolar North (e.g. Hugelius  
65 and Kuhry, 2009; Hugelius et al., 2010; Horwath Burnham and Sletten, 2010; Palmtag et al., 2015;  
66 Gentsch et al., 2015a; Siewert et al., 2016). Recent studies have also focused on re-evaluating the  
67 spatial extent and SOC storage of the Yedoma ‘Ice Complex’ and Alas deposits (Strauss et al., 2013;  
68 Walter-Anthony et al., 2014; Hugelius et al., 2016; Shmelev et al., 2017).

69 This new data has prompted an update of the total SOC storage in the northern permafrost  
70 region, its vertical partitioning and its broad (continental scale) distribution (Hugelius et al., 2014).  
71 The new estimate amounts to c. 1400 PgC for the top 3 m of soils and deeper deposits, including  
72 permafrost and non-permafrost organic soils (Histels/Histosols, 302 PgC), cryoturbated permafrost  
73 mineral soils (Turbels, 476 PgC), non-cryoturbated permafrost mineral soils (Orthels) and non-  
74 permafrost mineral soils (256 PgC), and deeper Yedoma (301 PgC, >300 cm) and Delta (91 PgC,  
75 >300 cm) deposits. The spatial distribution of SOC stocks according to the major permafrost soil  
76 (Gelisol) suborders, non-permafrost mineral soils and Histosols (Soil Survey Staff, 2010) is  
77 graphically represented in the updated version of the Northern Circumpolar Soil Carbon Database  
78 (NCSCDv2, 2014).

79 The importance of an accurate estimate of total SOC storage in the northern permafrost region is  
80 illustrated by a recent review of the permafrost carbon feedback (Schuur et al., 2015), which  
81 included a comparison of future C release in a total of eight Earth System models. The magnitude of  
82 the projected cumulative C loss from the permafrost region by 2100, largely based on the RCP 8.5  
83 scenario (IPCC, 2013), varied greatly between models from 37 to 174 PgC. However, by  
84 normalizing for the initial C pool size in the different models, the proportional C loss from the  
85 permafrost zone was constrained to a much narrower range of  $15 \pm 3$  % of the initial pool. This  
86 indicates that the quantity of SOC is a primary control when assessing C losses from the northern  
87 permafrost region.

88 The magnitude of the permafrost carbon feedback, however, will not only depend on the rate of  
89 future global warming (and its polar amplification), its effect on gradual and abrupt permafrost  
90 thawing (Grosse et al., 2011), or the total size (and vertical distribution) of the permafrost SOC pool.  
91 As shown by Burke et al. (2012), based on simulations with the Hadley Centre climate model,  
92 quality (decomposability) parameters need also to be considered. Thus, in terms of C pool  
93 parameters, the potential C release from the northern permafrost region will depend not only on SOC  
94 quantity but also on soil organic matter lability (i.e. the rate at which SOM will decay following  
95 warming and thawing). An important tool to assess potential C release from permafrost soils and

96 deposits are laboratory incubation experiments that consider both different types of substrate (e.g.,  
97 Schädel et al., 2014) and time of incubation (e.g. Elberling et al., 2013).

98 The aim of this study is to add a measure of SOM lability to the current estimates of SOC  
99 quantity, in order to define vulnerable C pools across the northern circumpolar region. We focus on  
100 the relationship between solid phase geochemical parameters (particularly C content) and C release  
101 rates in laboratory incubations of active layer and thawed permafrost samples from the main types of  
102 soils and deposits found in the northern permafrost region. Our objective is to develop a SOM  
103 lability classification scheme based on widely reported soil geochemical parameters in field SOC  
104 inventories and general landscape classes, that can be linked to existing spatial SOC databases such  
105 as the NCSCD (Tarnocai et al., 2009; Harden et al., 2012; Hugelius et al., 2014). We test the  
106 robustness of our SOM lability classification by comparing two very different types of incubation  
107 experiment, both in setup as well as timing of C release measurements.

108

## 109 2. Materials and methods

110

### 111 *2.1. Study areas*

112

113 The samples used in the incubation experiments were collected as part of landscape-level inventories  
114 carried out in the context of the EU PAGE21 and ESF CryoCarb projects to assess total storage,  
115 landscape partitioning and vertical distribution of SOC stocks in study areas across the northern  
116 permafrost region. SOC storage data from these areas are presented in Weiss et al. (2017) for  
117 Svalbard, Siewert et al. (2016) for Lena Delta, Palmtag et al. (2016) for Taymyr Peninsula, Palmtag  
118 et al. (2015) for Lower Kolyma, Hugelius et al. (2011) for Seida, and Siewert (2018) for Stordalen  
119 Mire. The location of all study areas is shown in Figure 1. The Lower Kolyma experiment includes  
120 samples from two nearby located study areas (Shalaurovo and Cherskiy); the Taymyr Peninsula  
121 experiment also includes samples from two nearby located study areas (Ary-Mas and Logata).  
122 Metadata for each of these areas, including geographic coordinates, permafrost and vegetation zones,  
123 climate parameters, number of soil profiles and incubated samples, type of incubation experiment,  
124 and time of field collection, are presented in Table S1 (Supplementary Materials).

125

126 Figure 1. Location of study areas in northern Eurasia. PAGE21 experiment (Ny Ålesund,  
127 Adventdalen, Stordalen Mire, Lena Delta); CryoCarb 1-Kolyma experiment (Shalaurovo,  
128 Cherskiy); CryoCarb 2-Taymyr experiment (Ary-Mas, Logata); CryoCarb 3-Seida experiment.  
129 Permafrost zones according to Brown et al. (1997).

130

### 131 *2.2. Field methods*

132

133 The sampling strategy applied for SOC field inventories was aimed at capturing all major landscape  
134 units in each of the study areas, while at the same time ensuring an unbiased selection of soil profile  
135 location. This semi-random sampling approach consisted of deciding on the positioning of generally  
136 1 or 2 km long transects that crossed all major landscape units, with a strictly equidistant sampling  
137 interval at normally 100 or 200 m that eliminated any subjective criteria for the exact location of  
138 each soil profile. For SOC storage calculations, the mean storage in each landscape unit class was  
139 weighed by its proportional representation in the study area based on remote sensing land cover  
140 classifications.

141 At each soil profile site, the topsoil organic layer was collected by cutting out blocks of known  
142 volume in three random replicates to account for spatial variability. These samples do not always

143 strictly adhere to the definition of an ‘O’ soil genetic horizon, because in areas with thin topsoil  
144 organics (like in floodplains and mountain terrain) there can be a large admixture of minerogenic  
145 material resulting in C contents of less than 12 %. Active layer samples were collected from  
146 excavated pits by horizontally inserting fixed-volume cylinders. The permafrost layer was sampled  
147 by hammering a steel pipe of known diameter incrementally into the ground, retrieving intact  
148 samples for each depth interval. Depths intervals are normally 5 to 10 cm or less (e.g., when the  
149 topsoil organic layer was very thin). The standard sampling depth was to 1 m below the soil surface;  
150 at some sites it was not possible to reach this depth due to large stones in the soil matrix or thin soil  
151 overlying bedrock (often in mountainous settings).

152

### 153 *2.3. Incubation experiments*

154

#### 155 **2.3.1. The PAGE21 incubation experiment**

156

157 The PAGE21 incubation experiment was carried out at the University of Copenhagen (Denmark).  
158 This experiment included one sample from the topsoil organics, one sample from the middle of the  
159 active layer and one sample from the upper permafrost layer (normally 10-15 cm below the upper  
160 permafrost table) from all mineral soil profiles collected in three of the PAGE21 study areas (Ny  
161 Ålesund, Adventdalen and Lena Delta). Samples were selected based on depth criteria and not any  
162 specific soil characteristic (e.g., presence of C-enriched cryoturbated material or absence of excess  
163 ground ice). In some cases, upper permafrost samples could not be collected due to very deep active  
164 layers and/or thin soils (particularly in mountain settings). Peat samples are available from a fourth  
165 PAGE21 study area (Stordalen Mire). In total c. 240 soil samples from four study areas across the  
166 northern permafrost region (Ny Ålesund and Adventdalen, Svalbard; Stordalen Mire, N Sweden;  
167 Lena Delta, N Siberia) were incubated in one and the same experiment (Faucherre et al., 2018).

168 The Dry Bulk Density (DBD) of samples used for incubation was measured at Stockholm  
169 University (Sweden). The %C and %N of dry weight of the incubated samples were measured in an  
170 elemental analyzer (EA Flash 2000, Thermo Scientific, Bremen, Germany) at the University of  
171 Copenhagen (Denmark).

172 Samples were kept in frozen condition from collection until the start of the laboratory incubation  
173 experiment. Samples were incubated at 5 °C and field water content levels (aerobic conditions) over  
174 a one-year time period. Mean volumetric water content varied between 30 % (topsoil organics), 45-  
175 50 % (active layer and permafrost layer mineral soil) and 69 % (peat). In the original PAGE21  
176 experiment (Faucherre et al., 2018), C-CO<sub>2</sub> production rates were measured at five different  
177 occasions between 7 to 343 days after the start of the experiment, using a nondispersive infrared LI-  
178 840A CO<sub>2</sub>/H<sub>2</sub>O Gas analyzer (LICOR® Biosciences). Since all samples from all study areas were  
179 processed and incubated using the same protocol, results are directly comparable. In this study, we  
180 use the C release rates on day 343 of incubation. These results, therefore, mostly address the ‘slow’  
181 (Schädel et al., 2014) and ‘stable’ (Knoblauch et al., 2013) SOM pools, with C cycling typically  
182 within a timespan of a (few) decade(s).

183

#### 184 **2.3.2. The CryoCarb incubation experiments**

185

186 The CryoCarb incubations were carried out at the University of South Bohemia (Ceske Budovice,  
187 Czech Republic). These experiments included all samples from all profiles collected in each of three  
188 study areas (CryoCarb 1-Kolyma in NE Siberia; CryoCarb 2-Taymyr in N Siberia; and CryoCarb 3-  
189 Seida in NE European Russia). In total c. 1000 samples were incubated.

190 The Dry Bulk Density (DBD) of samples used for incubation was measured at Stockholm  
191 University (Sweden). The %C and %N of dry weight were measured in an EA 1110 Elemental  
192 Analyzer (CE Instruments, Milan, Italy) at Stockholm University (Seida samples) and the University  
193 of Vienna (Kolyma and Taymyr samples).

194 The CryoCarb 1-Kolyma and CryoCarb-2 Taymyr samples were stored in a ground pit dug into  
195 the active layer for up to two weeks, before further processing. Active layer samples would be little  
196 impacted by this storage under ‘natural’ conditions, but (some of) the gradually thawing permafrost  
197 layer samples might have experienced initial decay. CryoCarb 3-Seida samples collected in 2009  
198 were kept in frozen storage for c. 10 years (see Table S1), before further processing.

199 In the laboratory, soil samples were dried at 40-50 °C within two weeks after field sampling (or  
200 retrieval from cold storage) and kept in a cold room (at 4 °C) until analyzed. For each sample, 0.2g  
201 of dry soil was inoculated with 0.003-0.008g of soil inoculum in 1.6 ml of water (soil : H<sub>2</sub>O, 1 : 100,  
202 weight/volume) in 10 ml vacutainers, after which the vacutainers were hermetically closed and the  
203 soil slurry was incubated in an orbital shaker at 12 °C for 96 hours. At the end of incubation, CO<sub>2</sub>  
204 concentration in the headspace was analyzed using an HP 5890 gas chromatograph (Hewlett-  
205 Packard, USA), equipped with a TC detector.

206 The study area and layer specific composite soil inoculi were prepared from fresh soil taken  
207 separately from topsoil organic layer, mineral active layer, peat active layer, mineral permafrost layer  
208 and peat permafrost layer, from multiple soil profiles collected in each study area. Fresh soil was  
209 kept in a cold room (at 4 °C) and then conditioned at 15 °C for one week before inoculum  
210 preparation. We consider that the small dry weight of our soil inoculi (which, in turn, have  $\leq 2$  %  
211 microbial biomass) has no significant impact on our C release measurements. The viability of inoculi  
212 was checked by incubation in water and measuring its respiration.

213 The short term C-CO<sub>2</sub> production rates measured in the CryoCarb experiments most likely  
214 address the ‘fast’ (Schädel et al., 2014) and ‘labile’ (Knoblauch et al., 2013) SOM pools, which  
215 represent a small fraction of the total pool and decompose within a (few) year(s). The CryoCarb  
216 approach is based on the so-called ‘Birch effect’ (Birch, 1958), showing that after a dry/wet cycle  
217 CO<sub>2</sub> mineralization increases. The extra C originates from mineralization of available C released  
218 from organo-mineral complexes and dead biomass. In our sample pretreatment with rapid drying at  
219  $\leq 50$  °C we expect that a larger part of biomass died and decomposed already during this process,  
220 which should therefore not severely affect our later measurements. Fierer and Schimel (2003)  
221 showed that a substantial part of the released C can also come from microbial biomass which died  
222 due to the osmotic shock after rewetting of soil. However, in their case samples were dried at room  
223 temperature resulting in less of a shock in the drying process to the microbial community. Our  
224 measurements could have been affected by limitation of C mineralization due to the small size of  
225 surviving biomass, which we overcame by inoculation with living cells. The principle of the ‘Birch  
226 Effect’ is still used in ecological studies ranging from large scale carbon cycling in ecosystems to  
227 detailed studies of SOC availability (e.g. Jarvis et al., 2007). It is well documented that the amount of  
228 extra C released after rewetting of dry soil is site and soil type specific and represents an easily  
229 available fraction of soil C (e.g. Franzluebbers et al., 2000; Šantrůčková et al., 2006). Due to  
230 different sample pretreatment, including duration until incubation experiment, as well as the different  
231 ‘local’ soil inoculi used, we consider the CryoCarb incubations of the three different study areas as  
232 separate experiments.

233

#### 234 *2.4. Geochemical parameters and C-CO<sub>2</sub> production rates*

235

236 As potential explanatory geochemical parameters we have considered dry bulk density (DBD),  
237 carbon content (%C of dry weight) and carbon to nitrogen weight ratios (C/N). In this study, we

238 focus on the relationship between %C in samples and the corresponding C-CO<sub>2</sub> production in  
239 aerobic incubation experiments. An important practical reason is that %C is most widely available  
240 since it can be derived with a high degree of confidence from Elemental Analysis, but also from  
241 indirect methods such as loss-on-ignition at 550 °C. However, there are also theoretical  
242 considerations for the choice of %C. DBD is expected to be related to quantity and degree of  
243 compaction (decomposition) of SOM. However, in the permafrost layer of soils it will also co-vary  
244 with the volume of excess ground ice. C/N is a good indicator of degree of SOM decomposition in  
245 peat deposits (Kuhry and Vitt, 1996) and tundra upland soils (Ping et al., 2008). Recent soil carbon  
246 inventories in permafrost terrain have shown a clear decrease in soil C/N as a function of age/depth  
247 (e.g., Hugelius et al., 2010; Palmtag et al., 2015). However, C/N is also sensitive to original botanical  
248 composition of the peat/soil litter. In contrast, the %C of plant material is much more narrowly  
249 constrained to around 50 % of dry plant matter. For instance, based on data in Vardy et al. (2000),  
250 we can calculate a C/N range of  $48.5 \pm 27.9$  (mean and standard deviation) in modern phytomass  
251 samples from permafrost peatlands in the Canadian Arctic (n=27) that included vascular plants,  
252 mosses and lichens. The corresponding %C range was much narrower at  $47.3 \pm 5.1$ . An additional  
253 benefit of using %C is that it has a clear ‘zero’ intercept in regressions against C-CO<sub>2</sub> production per  
254 gram dry weight per day (i.e., at zero %C in soil samples we can expect zero C release). This is also  
255 the reason why expressing C release as a function of gram dry weight (gdw) is more straightforward  
256 than against gram C (gC). The latter would have the benefit of expressing C release directly as a  
257 function of C stock, but the relationship is complex with recent studies showing high initial C release  
258 rates per gC at low %C values (Weiss et al., 2016; Faucherre et al., 2018). In this study DBD is  
259 available for all samples, and we can also express C release as a function of soil volume (cm<sup>3</sup>). In the  
260 results we primarily show  $\mu\text{gC-CO}_2$  production per gdw per day ( $\mu\text{gC-CO}_2 \text{ gdw}^{-1} \text{ d}^{-1}$ ) as a function  
261 of %C in the sample. However, in the Supplementary Materials we also refer to regressions against  
262 C/N and C-CO<sub>2</sub> production rates per gC per day ( $\mu\text{gC-CO}_2 \text{ gC}^{-1} \text{ d}^{-1}$ ) or per cm<sup>3</sup> of soil per day ( $\mu\text{gC-}$   
263  $\text{CO}_2 \text{ cm}^{-3} \text{ d}^{-1}$ ) against %C, to test the robustness of our results.

264

## 265 2.5. Landscape partitioning

266

267 We have investigated C-CO<sub>2</sub> production rates for the full datasets as well as for samples grouped  
268 into landscape unit classes that can be used for an assessment of vulnerable C pools at northern  
269 circumpolar levels. For this purpose, we have subdivided our datasets to reflect the main Gelisol  
270 suborders, non-permafrost mineral soils and Histosols recognized in the spatial layers of the  
271 NCSCD, as well as deeper Quaternary deposits for which there are separate estimates of spatial  
272 extent, depth and SOC stocks (Tarnocai et al., 2009; Strauss et al., 2013; Hugelius et al., 2014). We  
273 identify the following landscape classes: peat deposits (Histels, and some Histosols), peaty wetland  
274 deposits (mostly Histic Gelisols, peat layer <40 cm deep), mineral soils (Turbels and Orthels, and  
275 some non-permafrost mineral soils) in mountain and lowland settings, fluvial/deltaic (alluvial)  
276 deposits, and eolian/Pleistocene Yedoma deposits. Special attention is paid to the lability of SOM in  
277 Holocene peat deposits, in deeper C-enriched buried layers and cryoturbated pockets, and in  
278 Pleistocene Yedoma deposits. All main classes are represented in the PAGE21 and CryoCarb 1-  
279 Kolyma incubation experiments. The CryoCarb 2-Taymyr dataset lacks sites with eolian parent  
280 materials, whereas the CryoCarb 3-Seida dataset does not include soils formed into either alluvial or  
281 eolian deposits. Pleistocene Yedoma deposits are only represented in the CryoCarb 1-Kolyma  
282 experiment. We focus on results from the PAGE21 and CryoCarb 1-Kolyma experiments but present  
283 the main results from the two other experiments in Supplementary Materials. For a full overview of  
284 landscape unit class representation in each of the incubation experiments and study areas, see Table  
285 S2.

286 In addition, we have applied a further subdivision of landscape unit classes in the PAGE21  
287 experiment to allow a more detailed statistical analysis of the dataset and assess the role of  
288 minerogenic inputs, cryoturbation and peat accumulation in SOM lability. For this purpose, the  
289 eolian class is separated into actively accumulating deposits (Adventdalen) and Holocene soils  
290 formed into Pleistocene Yedoma parent materials (Lena Delta); Alluvial deposits are subdivided into  
291 profiles from active and pre-recent floodplains (multiple study areas); Mineral soils are separated  
292 into active colluviation sheets (mountain slopes on Svalbard) and other mineral soils (multiple study  
293 areas); Finally, for wetland deposits we discriminate between peat deposits (fens and bogs in  
294 Stordalen Mire; >40 cm peat) and peaty wetland profiles (multiple study areas, <40 cm peat). It  
295 should be stressed that these subclasses are not specifically recognized in any circumpolar SOC  
296 database and therefore of limited use for further upscaling. In all cases, SOM lability in samples of  
297 deeper C-enriched buried layers and cryoturbated pockets is shown for comparative purposes.

298

## 299 *2.6. Statistics*

300

301 Relationships between C-CO<sub>2</sub> production rates and geochemical parameters for all samples, as well  
302 as for groupings of samples into landscape unit classes, for each incubation experiment separately,  
303 are statistically analyzed using linear, polynomial and other non-linear regressions in the Microsoft  
304 Excel 2010 and Past3 (Hammer et al., 2001) software packages. Regressions are considered  
305 significant if  $p < 0.05$ . These analyses visualize SOM lability for full profiles including samples from  
306 topsoil organic to mineral layers that have a wide range of DBD, %C and C/N values. In some cases,  
307 replicates are not normally distributed (or even unimodal) and statistics should be interpreted with  
308 caution. This is particularly the case in peatland profiles, with clusters of samples with low DBD and  
309 high %C and C/N in the peat and opposite trends in samples of the underlying mineral subsoil.

310 To alleviate the issue on non-normal distributions, C-CO<sub>2</sub> production rates in samples as a  
311 function of %C are also tested grouped into soil horizons (PAGE21 and CryoCarb 1-Kolyma  
312 experiments). This approach yields classes that are much better constrained in terms of %C values.  
313 Because data were still not fully normally distributed, non-parametrical Mann-Whitney tests were  
314 used (Hammer et al., 2001). The data were log-transformed to reduce skewness in data distributions  
315 and to reduce the influence of fractional data. For the mineral soils in the PAGE21 incubation  
316 experiment, we differentiated between the topsoil organic layer, the active layer mineral soil, the  
317 permafrost layer mineral soil, and C-enriched pockets in both active layer and permafrost layer.  
318 Samples from topsoil organic layer, the active layer mineral soil and the permafrost layer mineral  
319 soil from profiles formed in Late Holocene loess deposits in Adventdalen (Svalbard) are considered  
320 separately, as are the active layer peat samples from Stordalen Mire (N Sweden). A similar grouping  
321 has been made for mineral soils in the CryoCarb 1-Kolyma experiment. In this case, Pleistocene  
322 Yedoma loess samples (both frozen and thawed) are considered separately. Peat samples are much  
323 better represented in the CryoCarb 1-Kolyma than PAGE21 experiment, and are subdivided into  
324 samples from thin peat layers in the active layer of peaty wetlands (Histic Gelisols), as well as  
325 samples from the active layer and permafrost layer of deep peat deposits (Histels). For this approach,  
326 we express C-CO<sub>2</sub> production rates per gC to take into account the large differences in %C among  
327 the different soil horizon classes. The tests are run to evaluate null hypotheses regarding differences  
328 in SOM lability between soil horizon classes, with a focus on those that are considered typical for  
329 specific landscape classes (C-enriched pockets for Turbels, peat samples for Histels and loess  
330 samples for Pleistocene Yedoma).

331

## 332 3. Results

333

334 *3.1. Simple geochemical indicators of SOM lability*

335

336 We first assessed the relationship between C release rates in incubation experiments and widely  
337 available physico-chemical parameters in samples from soil carbon inventories carried out  
338 throughout the northern permafrost region. The latter include dry bulk density (DBD), C content as a  
339 percentage of dry sample weight (%C), and carbon to nitrogen weight ratios (C/N). In recent studies  
340 dealing with incubation of soil samples from the northern permafrost region, %C and C/N of soil  
341 samples were highlighted as best parameters to predict C release (Elberling et al., 2013; Schädel et  
342 al., 2014). DBD was highlighted as a useful proxy in the recent synthesis of PAGE21 incubation  
343 studies presented in Faucherre et al. (2018). All three parameters are significantly (anti-)correlated  
344 with each other in the four different incubation experiments (Table 1 and Fig. S1). This can be  
345 expected, since organically enriched topsoil samples have low DBD, high %C and high C/N values  
346 compared to mineral layer soil samples. Also deeper soil samples, C-enriched through the process of  
347 cryoturbation (Bockheim, 2007), have generally relatively low DBD, high %C and high C/N values  
348 compared to adjacent mineral soil samples (e.g. Hugelius et al., 2010; Palmtag et al., 2015).

349

350 Table 1. R<sup>2</sup> values of cross correlations and number of samples (in brackets) between three  
351 geochemical parameters in the PAGE21 and three CryoCarb incubation experiments (all  
352 significant, p<0.05). For regression models see Figure S1.

353

354 All three considered geochemical parameters are significantly (anti-)correlated with measured C  
355 release rates in the four different incubation experiments. Lower DBD, higher %C and higher C/N  
356 values are associated with higher C-CO<sub>2</sub> production per gdw of the samples (Table 2 and Fig. S2).  
357 Of the three parameters, DBD explains most of the observed variability in C release in two  
358 experiments, whereas C/N shows highest R<sup>2</sup> values in the other two experiments.

359

360 Table 2. R<sup>2</sup> values of regressions and number of samples (in brackets) between three geochemical  
361 parameters and μgC-CO<sub>2</sub> production per gram dry weight in the PAGE21 and three CryoCarb  
362 incubation experiments (all significant, p<0.05). For regression models see Figure S2.

363

364 *3.2. Partitioning of the datasets based on landscape unit classes*

365

366 Our results show a significant relationship between μgC-CO<sub>2</sub> production per gdw as a function of  
367 %C of the soil sample for the full datasets in each of the four incubation experiments (Table 2 and  
368 Fig. S2). However, less than 50 % of the variability is explained by this relationship, which implies  
369 that it has limited usefulness to predict C release. The experiments show a large range in μgC-CO<sub>2</sub>  
370 production per gdw, particularly at medium to high %C values. In this section we analyze whether a  
371 grouping of samples according to landscape unit classes can disentangle some of the observed  
372 variability.

373 Figure 2 shows the relationships between C release rates and %C in the samples for the data  
374 grouped according to major landscape unit classes in the PAGE21 (measured on day 343 of  
375 incubation) and CryoCarb 1-Kolyma (measured over the first four days of incubation) experiments.  
376 For the sake of simplicity, we apply linear regressions with intercept zero to all classes. These are  
377 identified by different colors and symbols that have been consistently used in Figures 2-3 and S3-S5.  
378 The regression for the full data set is provided as reference (dotted lines), but it should be noted that  
379 its slope is partly determined by the number of samples in each of the recognized landscape units.

380

381 Figure 2.  $\mu\text{gC-CO}_2$  production per gram dry weight as a function of %C of the sample for the full  
382 datasets and different landscape classes in the longer-term PAGE21 (a, top panel) and short-  
383 term CryoCarb 1-Kolyma (b, lower panel) incubation experiments: All samples (dotted grey  
384 lines); Alluvial class (red line and diamonds); Eolian class (blue line and triangles); Mineral class  
385 (brown line and squares); Peaty wetland class (dark green line and circles); Peatland class (light  
386 green line and circles). All regressions significant ( $p < 0.05$ ), except for the PAGE21 peatland  
387 class (n.s.).

388

389 A first observation is that C release rates per gdw are c. 15 times lower in the longer-term  
390 PAGE21 experiment compared to the short-term CryoCarb 1-Kolyma experiment. In the PAGE21  
391 dataset (Fig. 2a), the soils developed into alluvial and eolian deposits and in peaty wetlands all show  
392 similar and relatively high SOM lability. Mineral soils show intermediate values, whereas the peat  
393 deposits display low SOM lability (when considering %C values). All regressions are significant,  
394 except for 'peat deposits' due to very high variability in three surface peat samples (but see Fig. 3d).  
395 In the CryoCarb 1-Kolyma data set (Fig. 2b), alluvial and eolian soils/deposits show the highest  
396 SOM lability, followed by mineral soils. In this case, peaty wetlands show a slightly lower lability  
397 than mineral soils/deposits but still considerably higher than peatlands. This clear dichotomy in the  
398 SOM lability of mineral soils (including peaty wetlands) and peat deposits is also apparent from the  
399 CryoCarb 2-Taymyr and CryoCarb 3-Seida results even though not all landscape classes are  
400 represented in those experiments (Fig. S3). The explanatory power of the regressions ( $R^2$  values) in  
401 the peatland class is generally lower than that in the mineral soil/deposit classes. These statistics are,  
402 however, greatly improved when removing the surface peat samples from the analyses (not shown),  
403 which display very high variability.

404 Linear regression analyses between C-CO<sub>2</sub> production per gdw and C/N ratios for all four  
405 experiments (Fig. S4) show small deviations from the above patterns but generally maintain the clear  
406 difference between 'peat deposits' and the remaining landscape units. However, C-CO<sub>2</sub> production  
407 was similar in peat deposits and mineral soils/deposits at low C/N values ( $\leq 20$ ).  $R^2$  values for the  
408 landscape classes are generally lower than in regressions against %C and regression lines at low C  
409 release tend to converge to C/N values of 8-12, which are typical for microbial decomposer biomass  
410 suggesting only slow internal cycling of remaining SOM (Zechmeister-Boltenstern et al., 2015).

411 The PAGE21 dataset with C-CO<sub>2</sub> production rates expressed per gC as a function of %C of the  
412 soil sample also shows similar results, however, with generally lower  $R^2$  and sometimes non-  
413 significant regressions (Fig. S5a). The same patterns are also noted when expressing C release as a  
414 function of soil volume ( $\text{cm}^3$ ), however,  $R^2$  values are generally even lower and more often non-  
415 significant (Fig. S5b).

416

### 417 3.3. Further subdivision of landscape unit classes in the PAGE21 dataset

418

419 Figure 3a-c, presents SOM lability in a further subdivision of the mineral soil/deposit landscape  
420 classes in the PAGE21 dataset. We have compared profiles with active accumulation/movement in  
421 eolian, alluvial and colluvial settings, with Holocene soils developed into older eolian, alluvial or  
422 other mineral parent materials, respectively. In each of these comparisons, we specifically identify  
423 samples from deeper C-enriched buried layers and cryoturbated pockets. Generally speaking, a  
424 second order polynomial (intercept zero) provides the best fit and has been applied for the sake of  
425 uniformity to all described subclasses. All these datasets have in common that the subclasses with  
426 active surface accumulation/movement have topsoil samples that show relatively low C content due  
427 to the continuous admixture of minerogenic materials. At the same time, these all show the highest  
428 C-CO<sub>2</sub> production per gdw (when considering %C). Furthermore, the second order polynomial

429 regressions of all subclasses (except for buried C-enriched samples) suggest that the topsoil samples  
430 are particularly labile suggesting the presence of a more degradable SOM pool in the recently  
431 deposited plant litter. Deeper C-enriched material shows relatively low lability and does not show  
432 rapidly increasing lability at higher %C values.

433 Figure 3d compares the SOM lability in fen and bog deposits (Stordalen Mire) and peaty  
434 wetland profiles (multiple study areas), adding for comparison the results from the previously  
435 described deeper C-enriched buried layers and cryoturbated pockets in mineral soils (see Figs. 3a-c).  
436 In this case, exponential functions best describe observed trends and indicate very high lability of  
437 surface peat(y) samples. The thin peat layers in peaty wetlands have relatively low %C values  
438 pointing to admixture of minerogenic materials. The SOM in these profiles show relatively high C-  
439 CO<sub>2</sub> production per gdw compared to 'true' peat samples (when considering %C). Compared to the  
440 non-significant linear regression for all peat samples shown in Figure 2a, exponential regressions for  
441 the peatland class as a whole as well as for fens and bogs separately are statistically significant.  
442 Particularly in fen peat, this regression is able to capture some very high C release values of two  
443 surface peat samples (corresponding to graminoid-derived plant litter). Deeper C-enriched material  
444 in mineral soils displays only slightly higher SOM lability compared to the mineral subsoil  
445 underlying peat deposits. It is important to bear in mind that the total number of peat samples from  
446 Stordalen Mire is limited (n=13) and that results cannot be compared directly to adjacent mineral soil  
447 profiles because field sampling in that particular study area focused solely on the peatland area.

448

449 Figure 3.  $\mu\text{gC-CO}_2$  production per gram dry weight as a function of %C of the sample for different  
450 landscape classes and their subdivisions in the PAGE21 incubation experiment. (a) Eolian class  
451 separated into actively accumulating deposit (light blue), Holocene soil formation into  
452 Pleistocene Yedoma parent materials (dark blue) and buried C-enriched samples (pink); (b)  
453 Alluvial class separated into active floodplain (rose), Holocene soil formation into pre-recent  
454 floodplain deposits (red) and buried C-enriched samples (pink); (c) Mineral class separated into  
455 active colluviation sheets (light brown), other mineral soils (dark brown) and one buried C-  
456 enriched sample (pink); (d) Wetland class separated into wetlands with thin peat layers (green),  
457 fens (light green) and bogs (dark green) with deep peat deposits and, for comparison, buried C-  
458 enriched samples in mineral soils (pink). The hatched line represents the regression for all  
459 peatland samples (fens and bogs) together. C-release from one surface peat sample (X) in the  
460 margin of a peatland is also indicated, but not included in the regressions. All regressions are  
461 significant ( $p < 0.05$ ).

462

#### 463 3.4. C-enriched cryoturbated and Pleistocene Yedoma samples in the CryoCarb 1-Kolyma dataset

464

465 In the PAGE21 incubation each collected profile included only one sample from the mineral soil in  
466 the middle of the active layer and one sample from the upper permafrost layer. Thus, the selection of  
467 samples was based on depth-specific criteria. As a result, the number of samples from deeper C-  
468 enriched buried layers and cryoturbated pockets is limited (n=13). In the CryoCarb 1-Kolyma  
469 experiment samples from entire profiles were incubated and the number of deeper C-enriched  
470 samples in the mineral soil horizons is much larger. Figure 4a compares the C-CO<sub>2</sub> production per  
471 gdw from organically-enriched topsoil and mineral soil samples not affected by C-enrichment with  
472 that in deeper C-enriched cryoturbated samples in tundra profiles. For the sake of clarity, only those  
473 cryoturbated samples which are C-enriched by at least twice the adjacent mineral soil %C  
474 background values are included (n=22). It should be emphasized that the actual absolute %C values  
475 for the C-enriched samples and mineral soil samples not affected by C-enrichment can vary between  
476 study areas and profiles, among others due to differences in soil texture (Palmtag and Kuhry, 2018).  
477 The results from this much more narrowly defined dataset are similar to those presented for the

478 PAGE21 experiment, i.e. SOM in deeper C-enriched cryoturbated samples is less labile than in  
479 organically-enriched topsoil samples with similar %C.

480 The PAGE21 experiment does not include any samples from Pleistocene Yedoma deposits. In  
481 contrast, the CryoCarb 1-Kolyma dataset has samples from two Yedoma exposures along river and  
482 thermokarst lake margins. The material was collected from perennially frozen Yedoma deposit as  
483 well as from thawed out sections of the exposures. C-release from these samples are presented in  
484 Figure 4b, which for comparison also shows samples from Holocene lowland soils, mineral subsoil  
485 samples beneath peat deposits and deeper C-enriched cryoturbated samples. The C-CO<sub>2</sub> production  
486 per gdw of Pleistocene Yedoma is lower than that of Holocene lowland soils, but somewhat higher  
487 than that of mineral subsoil beneath peat and deeper C-enriched material (when considering %C).  
488 Furthermore, the SOM lability of thawed out deposits is somewhat lower than that of the intact  
489 permafrost Yedoma material.

490

491 Figure 4.  $\mu\text{gC-CO}_2$  production per gram dry weight as a function of %C of the sample in the  
492 CryoCarb 1-Kolyma incubation experiment for (a) Deeper C-enriched samples (pink line and  
493 triangles), compared to samples of organically enriched topsoil and mineral soil not affected by  
494 C-enrichment in all tundra profiles (blue line and triangles, showing lower part of regression  
495 line), and for (b) Perennially frozen Pleistocene Yedoma samples (black line and triangles) and  
496 thawed out Pleistocene Yedoma samples (red line and triangles), compared to samples of  
497 organically enriched topsoil and mineral soil not affected by C-enrichment in Holocene lowland  
498 profiles (blue line and triangles, showing start of regression line), mineral subsoil samples  
499 beneath peat deposits (green line and circles, showing start of regression line) and buried C-  
500 enriched samples (pink line and triangles, showing start of regression line). All regressions  
501 (power fit) are significant ( $p < 0.05$ ).

502

### 503 3.5. Relative lability ranking of SOM landscape unit classes

504

505 Table 3a shows the slopes of the linear regressions (intercept zero) between C-CO<sub>2</sub> production per  
506 gdw and %C of samples for the different landscape unit classes in all four incubation experiments.  
507 From these results it is clear that results from the four experiments cannot be compared directly in  
508 quantitative terms. To facilitate comparison across experiments results were normalized to the  
509 lowland mineral soil class, which consistently showed intermediate SOM labilities. Table 3b shows  
510 the normalized regression slopes (with the slope for mineral soils set to 1), and their mean and  
511 standard deviation (when the landscape class is represented in more than one incubation experiment).  
512 This approach confirms the previous results that peat deposits and deeper C-enriched samples in  
513 mineral soils consistently show very low relative lability, whereas areas with recent mineral sediment  
514 accumulation (e.g. in recent eolian deposits) display generally somewhat higher SOM lability (when  
515 considering %C). Pleistocene Yedoma deposits, only represented in one incubation experiment, also  
516 display relative low SOM lability.

517

518 Table 3. (a) Slopes of linear regressions (intercept zero) between %C and C-CO<sub>2</sub> production per gdw  
519 in samples of the different landscape classes in the four experiments; (b) Normalized slopes of  
520 linear regressions between %C and C-CO<sub>2</sub> production per gdw for samples in the different  
521 landscape classes in the four experiments (slope of mineral soils in lowland settings set to 1).  
522 Abbreviations: 'Pt' = peat deposits (Histels/Histosols), excluding two surface graminoid litter  
523 samples (PAGE21, Stordalen Mire); 'Min/CE' = C-enriched pockets in cryoturbated soils  
524 (Turbels); 'Min Mtn' = mineral soils in mountain settings; 'Min Pty' = peaty wetlands (mineral  
525 soils with histic horizon); 'Min Lowl' = mineral soils in lowland settings; 'Alluv' = recent alluvial

526 deposits and Holocene soils formed in alluvial deposits; 'Eol' = recent eolian deposits; 'Pl Yed' =  
527 Pleistocene Yedoma deposits.

528

### 529 3.6. SOM lability based on soil horizon criteria

530

531 We also tested SOM lability in samples grouped according to soil horizon criteria (PAGE21 and  
532 CryoCarb 1-Kolyma experiments), with special attention to those horizon classes that can be linked  
533 to the specific landscape classes showing low relative SOM lability (C-enriched pockets for Turbels,  
534 peat samples for Histels and loess samples for Pleistocene Yedoma). This approach yielded classes  
535 with data distributions that are much better constrained in terms of %C values.

536 In this analysis we focus on C-CO<sub>2</sub> production per gC to take into account large differences in  
537 %C between soil horizon classes (see Fig. S6). The main difference between the two experiments is  
538 the much lower %C values of the topsoil organic class in the PAGE21 incubation, which can be  
539 explained by a greater surface admixture of minerogenic material in alluvial (Lena Delta), eolian and  
540 mountainous areas (Svalbard). In contrast, the predominant lowland setting of the CryoCarb 1-  
541 Kolyma study area is characterized by soils with thicker, more C-rich, topsoil organic layers.

542 Figure 5 shows C-CO<sub>2</sub> production per gC in the soil horizon groups of the longer term PAGE21  
543 and short-term CryoCarb 1-Kolyma experiments. Results of the Mann-Whitney paired tests for both  
544 these experiments are shown in Table 4. PAGE21 classes show fewer statistically significant  
545 differences than in the CryoCarb 1-Kolyma experiment, which can at least partly be ascribed to  
546 smaller sample sizes. The number of samples in the PAGE21 incubation for C-enriched pockets in  
547 the active layer (n=3) and for peat (n=6) are particularly low.

548

549 Figure 5.  $\mu\text{gC-CO}_2$  production per gram carbon in samples of (a) the PAGE21 and (b) the CryoCarb  
550 1-Kolyma incubation experiments, grouped according to soil horizon criteria. Abbreviations:  
551 AL-OL = Active layer topsoil organics; AL-Min = Active layer mineral; AL-Ce = Active layer  
552 C-enriched; P-Min = Permafrost layer mineral; P-Ce = Permafrost layer C-enriched; AL-Pty =  
553 Active layer thin peat (CryoCarb 1-Kolyma experiment only); AL-Pt = Active layer peat; P-Pt =  
554 Permafrost layer peat (CryoCarb 1-Kolyma experiment only); AL-Lss OL = Active layer topsoil  
555 organics in Late Holocene loess deposits (PAGE21 experiment only); AL-Lss Min = Active  
556 layer mineral in Late Holocene loess deposits (PAGE21 experiment only); P-Lss Min =  
557 Permafrost layer mineral in Late Holocene loess deposits (PAGE21 experiment only); Fr-Yed =  
558 Permafrost Pleistocene Yedoma deposits (CryoCarb 1-Kolyma experiment only); Th-Yed =  
559 Thawed out Pleistocene Yedoma deposits (CryoCarb 1-Kolyma experiment only). Box-whisker  
560 plots show mean and standard deviation (in red) and median, first and third quartiles and  
561 min/max values (in black), for the different soil horizon groups.

562

563 Table 4. p Values of Mann-Whitney paired tests of  $\mu\text{gC-CO}_2$  production per gram carbon for soil  
564 horizon groups in (a) the PAGE21 and (b) the CryoCarb 1-Kolyma incubation experiments.  
565 Abbreviations as in Figure 5. Differences are considered significant when  $p < 0.05$ .

566

567 C release rates in topsoil organic samples from actively accumulating Holocene loess soils are  
568 significantly higher than those in topsoil organic samples from the remaining PAGE21 mineral soils  
569 (Fig. 5a and Table 4a). Both topsoil organic classes show significantly higher rates than all mineral  
570 soil and peat classes. Peat samples have the lowest mean and median C release rates from all these  
571 classes but only the rates from permafrost layer mineral soil and C-enriched pocket samples are  
572 significantly higher. Both mean and median C release rates from active layer and permafrost layer C-

573 enriched pockets are somewhat lower (but not significantly different) than those from adjacent, non  
574 C-enriched, mineral soil samples.

575 C release rates in the soil horizon classes from the CryoCarb 1-Kolyma experiment show  
576 similarities, but also some differences to those observed in the PAGE21 experiment. Absolute C  
577 release rates per gC are more than an order of magnitude higher in the CryoCarb 1-Kolyma  
578 experiment (measured as a mean release over the first four days of incubation) compared to those in  
579 the PAGE21 experiment (measured on day 343 of incubation). Another important difference is that  
580 C release rates per gC in the short-term CryoCarb 1-Kolyma incubation do not differ significantly  
581 between the topsoil organic class and the active layer and permafrost layer mineral soil classes,  
582 which we ascribe to the presence of a highly labile C pool (e.g. DOC, plant roots) in the mineral soil  
583 layers that is quickly decomposed (see Weiss et al., 2016; Faucherre et al., 2018). However, rates  
584 from active layer and permafrost layer C-enriched pockets are significantly lower than those from  
585 adjacent, non C-enriched, mineral soil samples. Both active layer and permafrost layer peat samples  
586 show significantly lower C release rates than all other classes, with active layer peat samples having  
587 significantly higher rates than permafrost layer peat samples. Samples from the Pleistocene Yedoma  
588 loess 'frozen' and 'thawed' classes display significantly lower C release rates per gC than those in  
589 the topsoil organic layer, active layer and permafrost layer mineral soil classes, but significantly  
590 higher rates than those in the peat classes. The two Yedoma classes do not differ significantly from  
591 each other, the active layer and permafrost layer C-enriched pocket classes, nor the peaty wetland  
592 class.

593

#### 594 4. Discussion

595

596 The analysis and comparison of results in the PAGE21 and CryoCarb 1-Kolyma incubations show  
597 consistent trends in C-CO<sub>2</sub> production rates as a function of simple soil geochemical parameters in  
598 both the full datasets as well as in the grouping of samples according to landscape classes. However,  
599 it is not possible to directly compare these two very different laboratory experiments quantitatively.  
600 The varying field collection techniques, field storage, transport and laboratory storage, pretreatment,  
601 experimental setup and time of measurement after start of incubations have a clear effect on the  
602 magnitude of the observed C-CO<sub>2</sub> production rates. The same methods were applied to all samples  
603 from all study areas in the PAGE21 experiment, but these differed markedly from those applied in  
604 the CryoCarb setup and even between the three individual CryoCarb experiments (e.g., addition of  
605 different 'local' microbial decomposer inoculi to rewetted samples).

606 In quantitative terms, C-CO<sub>2</sub> production rates per gdw measured over the first 4 days in the  
607 CryoCarb 1-Kolyma samples incubated at 12 °C are about 15 times higher than those measured after  
608 about one year in the PAGE21 samples incubated at 5 °C (see Fig. 2). Similarly, C-CO<sub>2</sub> production  
609 rates per gC are also more than an order of magnitude higher in the short-term CryoCarb-Kolyma 1  
610 than the longer term PAGE21 incubation (see Fig. 5). Upper permafrost mineral soil samples (<3  
611 %C) from Kylatyk in NE Siberia, incubated at 2 °C directly after field collection and thawing  
612 (measurement after 20-30 hr, following 3 days of pre-incubation), show median C release rates of c.  
613 750 μgC-CO<sub>2</sub> gC<sup>-1</sup> d<sup>-1</sup> (Weiss et al., 2016), compared to c. 1750 μgC-CO<sub>2</sub> gC<sup>-1</sup> d<sup>-1</sup> in the same class  
614 of CryoCarb 1-Kolyma samples. Median C release rates in upper permafrost mineral soil samples of  
615 the PAGE21 experiment (Faucherre et al., 2018) decrease from c. 170 on day 8 to c. 35 μgC-CO<sub>2</sub>  
616 gC<sup>-1</sup> d<sup>-1</sup> on day 343 since start of incubation. It is obvious from these results that there is a rapid  
617 decline in C release rates over time of incubation. Longer incubation experiments (up to 12 years)  
618 have shown that the overall rate of C loss decreases almost exponentially over time (Elberling et al.,  
619 2013). However, even when laboratory incubation setups and time of measurement are similar, large  
620 differences can occur in C release rates. For instance, peat samples in the CryoCarb 1-Kolyma

621 incubation display about twice the C-CO<sub>2</sub> production rates per gdw than those observed in the  
622 CryoCarb 3-Seida incubation (Figs. 2b and S3b).

623 Nonetheless, a comparison of C-CO<sub>2</sub> production rates per gdw for landscape unit classes in  
624 terms of relative SOM lability provided useful and robust results. These classes were implemented to  
625 allow upscaling of results to the northern permafrost region. They reflect main Gelisol (and non-  
626 Gelisol) soil suborders and deeper Quaternary deposits to permit direct comparison with the size and  
627 geographic distribution of these different SOC pools (Tarnocai et al., 2009; Hugelius et al., 2014).  
628 Samples from mineral soil profiles, including wetland deposits with a thin peat(y) surface layer,  
629 display high relative SOM lability compared to peat deposits, deep C-enriched buried or cryoturbated  
630 samples and Pleistocene Yedoma deposits (when considering %C of the incubated sample). These  
631 results are confirmed by the more stringent statistical analysis of samples grouped into soil horizon  
632 classes. Peat deposit, C-enriched pocket and Yedoma deposit samples show significantly lower C-  
633 CO<sub>2</sub> production rates per gC than topsoil organics and mineral layer samples (Cryo-Carb-1-Kolyma  
634 experiment). The same trends are observed in the incubation experiment of upper permafrost samples  
635 from Kytalyk, reported by Weiss et al. (2016). C-enriched pockets (3-10 %C) showed lower C-CO<sub>2</sub>  
636 production rates per gC than mineral soil samples (<3 %C), while a buried peat sample (c. 40 %C)  
637 displayed a very low C-CO<sub>2</sub> production rate per gC. The PAGE21 experiment also revealed that peat  
638 samples mineralized a smaller fraction of C over the one year of incubation compared to mineral soil  
639 samples (Faucherre et al., 2018).

640 A further subdivision of landscape classes and more careful analysis of incubation results in the  
641 PAGE21 experiment provide additional useful insights. For example, separation of eolian deposits  
642 into actively accumulating deposits during the Late Holocene (Adventdalen) and Holocene soils  
643 formed into Pleistocene Yedoma parent materials (Lena Delta) showed clear differences in C release  
644 rates per gdw (when considering %C), with the former displaying a higher SOM lability in topsoil  
645 organic samples (see Fig. 3a). The topsoil organic samples from the actively accumulating eolian  
646 deposits in Adventdalen also displayed significantly higher C release rates per gC than all other  
647 topsoil organic, mineral layer and peat(y) horizon classes (see Table 4a). Separation of alluvial  
648 deposits into active floodplain deposits and Holocene soils formed in pre-recent river terraces and of  
649 mineral soils into active colluviation sheets (mountain slopes on Svalbard) and other mineral soils  
650 showed similar trends in SOM lability (see Fig. 3b-c). These results suggest that admixture of  
651 minerogenic material in topsoil organics of actively accumulating eolian, alluvial and colluvial  
652 deposits promotes SOM decomposition. Peaty wetland deposits display much higher C release rates  
653 per gdw (when considering %C) than peatland deposits (see Fig. 3d). These two landscape classes  
654 are poorly represented in the PAGE21 experiment, but a statistical test of C release rates per gC in  
655 these peat(y) soil horizon classes of the CryoCarb 1-Kolyma incubation confirms this difference (see  
656 Table 4b). This is interesting because even though wetlands with a thin peat layer do not have  
657 particularly high C stocks, they can be important sources of methane (CH<sub>4</sub>) to the atmosphere  
658 (Olefeldt et al., 2013). These further subdivisions into landscape subclasses are of limited use for  
659 upscaling purposes because they are not considered explicitly in any available geographic database  
660 for the northern permafrost region.

661 The implementation of landscape classes (and their subdivisions) in the PAGE21 and CryoCarb  
662 incubation experiments have greatly constrained variation in C release rates compared to the full  
663 datasets. However, much within-class variability remains and there is a need to further investigate  
664 the sources of this variability. Important additional soil and environmental factors such as microbial  
665 community, moisture, texture, pH, redox potential, etc. were not available for the (full) PAGE21 and  
666 CryoCarb datasets and could, therefore, not be tested. We conclude that additional research is needed  
667 to further constrain observed SOM lability across the northern permafrost region and within the  
668 classes proposed here.

669 The relatively low lability in the peatland class is surprising. The low DBD, high %C and high  
670 C/N of peat are normally associated with a relatively low degree of decomposition. This, in turn, is  
671 the result of environmental factors such as anaerobic and/or permafrost conditions that largely inhibit  
672 SOM decay (Davidson and Janssens, 2006). One could expect that this less decomposed material  
673 would show high lability following thawing and warming, but our results point to the opposite. This  
674 is particularly surprising when considering the setup of the CryoCarb experiments, in which a slush  
675 of rewetted material inoculated with microbial decomposers was incubated at 12 °C. Although the  
676 CryoCarb experiments are very short assays (4 days), the longer term PAGE21 incubation data  
677 (measured after roughly one year) provides similar results.

678 In the case of peat deposits, it should be considered if this low decomposability is an evolved  
679 ‘biochemical trait’ in peat-forming species that maintains their favored habitat, similar to the role of  
680 *Sphagnum* anatomy (hyaline cells), physiology (acidification) and cell wall chemistry (phenolic  
681 compounds) in sustaining moist and acid surface conditions, and inhibiting peat decomposition  
682 (Clymo and Hayward, 1982). Furthermore, the generally high C/N ratios of peat provide a poor  
683 substrate quality to the decomposer community (Bader et al., 2018). Diáková et al. (2016) reported  
684 low microbial biomass in subarctic peat deposits of the Seida study area (Northeast European  
685 Russia). Permafrost degradation in peatlands can result in two opposite pathways, one resulting in  
686 surface collapse and an increase in soil moisture (particularly mimicked in the CryoCarb incubation  
687 setup) and another one resulting in drainage, drying and accelerated C losses, not the least due to a  
688 higher incidence of peat fires (Kuhry, 1994).

689 Our results on the low lability of peat deposits can be compared to the findings of Schädel et al.  
690 (2014) in their assessment of SOM decomposability in the northern permafrost region. That study  
691 recognized a group of organic soil samples (>20% initial C), ranging in depth between 0 and 120 cm.  
692 We consider that this group will include both topsoil organic samples as well as deeper peat deposits.  
693 In the Schädel et al. (2014) study, this group showed the largest range in decomposability, with some  
694 samples showing high potential C losses, whereas deeper organic samples were less likely to respire  
695 large amounts of C. We suggest, therefore, that both studies might show the same trends.

696 In our incubation experiments, SOM from deeper C-enriched buried layers and cryoturbated  
697 pockets show relatively low lability when compared to organic-rich topsoil samples. These results  
698 are corroborated by Čapek et al. (2015) and Gentsch et al. (2015b), who report low bioavailability of  
699 SOM in subducted horizons of Lower Kolyma soils (NE Siberia). The reason why this relatively  
700 undecomposed material displays low lability remains unclear. One reason could be that the  
701 decomposer community needs time to adapt to the new environmental conditions following  
702 thawing/warming, another one that there is a simple mismatch between the microbial community  
703 adapted to decompose relatively undecomposed organic material and the physico-chemical  
704 environment (e.g., higher bulk density) prevailing in (thawed out) deeper soil horizons (Gittel et al.,  
705 2013; Schnecker et al., 2014). Kaiser et al. (2007) and Čapek et al. (2015) reported low microbial  
706 biomass in deeper C-enriched soil samples.

707 These results pose interesting questions regarding the role of organic aggregates and organo-  
708 mineral associations for SOM lability (e.g. Gentsch et al., 2018). On the one hand, our samples from  
709 topsoil organic horizons with active minerogenic inputs in eolian, alluvial and colluvial settings  
710 display (very) high C release rates, whereas deeper C-enriched soil materials show low  
711 decomposability. The underlying soil physico-chemical and microbial processes require urgent  
712 attention in order to better constrain C release rates from soils and deposits in the northern  
713 permafrost region.

714 Pleistocene Yedoma deposits, represented in the CryoCarb 1-Kolyma incubation experiment,  
715 also display low relative SOM lability, despite incorporation of relative fresh plant root material  
716 caused by syngenetic permafrost aggradation. These results are corroborated by results from Schädel  
717 et al. (2014) for their group of deep mineral samples (with Yedoma provenance).

718 An important consideration is if the consistent differences in relative SOM lability of landscape  
719 and soil horizon classes observed in our incubation experiments will be maintained over periods of  
720 decades to centuries of projected warming and thawing. Very short-term incubations, such as in the  
721 CryoCarb setup (four days), might register the initial decomposition of highly labile SOM  
722 components, such as microbial necromass, simple molecules (e.g., sugars or amino acids), low  
723 molecular-weight DOC, etc., or might not provide enough time for an adaptation of the microbial  
724 decomposer community to new environmental settings (Weiss et al., 2016; Weiss and Kaal, 2018).  
725 On the other hand, in longer incubation experiments such as in the PAGE21 experiment (one year),  
726 the conditions in the incubated samples become gradually more artificial compared to field  
727 conditions. Specifically, microbes in long-term incubations become increasingly C limited, as no  
728 new C input by plants occur, whereas inorganic nutrients, such as nitrate or ammonium accumulate  
729 to unphysiological levels. Care, therefore, should be taken when extrapolating our results over longer  
730 time frames if no corroborating field evidence for longer term decay rates can be obtained (e.g.  
731 Kuhry and Vitt, 1996; Schuur et al., 2009).

732

## 733 5. Conclusions

734

735 The PAGE21 and CryoCarb incubation experiments confirm results from previous studies that  
736 simple geochemical parameters such as DBD, %C and C/N can provide a good indication of SOM  
737 lability in soils and deposits of the northern permafrost region (Elberling et al., 2013; Schädel et al.,  
738 2014; Faucherre et al., 2018). In our analyses we have focused on %C of the sample since it is the  
739 most widely available of the three investigated geochemical parameters. Furthermore, %C is less  
740 sensitive than C/N to botanical origin of the plant litter and, in contrast to DBD, not dependent on  
741 ground compaction or volume of excess ground ice.

742 When considering the full datasets of the four experiments, our regressions of C release as a  
743 function of %C were statistically significant but explained less than 50 % of the observed variability.  
744 Subsequently, we investigated whether a further division of samples into predefined landscape unit  
745 classes would better constrain the observed relationships. In defining these classes, we applied a  
746 scheme that could easily be used for spatial upscaling to northern circumpolar levels. We adopted the  
747 main Gelisol suborders (Histels, Turbels and Orthels), non-permafrost Histosols and mineral soils,  
748 and types of deeper Quaternary (deltaic/floodplain and eolian/Yedoma) deposits that have been used  
749 in the NCSCD and related products to estimate the total SOC pool in the northern permafrost region  
750 (Tarnocai et al., 2009; Strauss et al., 2013; Hugelius et al., 2014). We conclude that these landscape  
751 classes better constrain observed variability in the relationships and that the relative SOM lability  
752 rankings of these classes were consistent among all four incubation experiments, for both regressions  
753 against %C and C/N (all four experiments), and for regressions of %C against different units of C-  
754 CO<sub>2</sub> production '*per gram dry weight*', '*per gram C*' and '*per cm<sup>3</sup>*' (PAGE21 dataset). Our results  
755 based on full profiles indicate that C-CO<sub>2</sub> production rates per gdw decrease in the order Late  
756 Holocene eolian > alluvial and mineral (including peaty wetlands) > Pleistocene Yedoma > C-  
757 enriched pockets > peat, with lowest C release rates observed in peat deposits (when considering  
758 %C). These results are corroborated by statistical analysis of C release rates per gC for samples  
759 grouped according to soil horizon criteria (PAGE21 and CryoCarb 1-Kolyma datasets).

760 An important conclusion from these results is that purportedly more undecomposed SOM, such  
761 as in peat deposits (Histels and Histosols), C-enriched cryoturbated samples (Turbels), and  
762 Pleistocene Yedoma deposits, does not seem to imply higher SOM lability. These three SOC pools,  
763 which together represent  $\geq 50$  % of the reported SOC storage in the northern permafrost region  
764 (Hugelius et al., 2014; Palmtag and Kuhry, 2018), display relatively low rates of C release.  
765 Consequently, there is an urgent need for further research to understand these results in order to  
766 better constrain the thawing permafrost carbon feedback on global warming.

767

## 768 6. Data availability

769

770 The soil geochemical data and incubation results presented in this paper are available upon request  
771 from PK (peter.kuhry@natgeo.su.se). For full PAGE21 incubation data, please contact BE  
772 (be@ign.ku.dk). For full CryoCarb incubation data, please contact JB (jiri.barta@prf.jcu.cz).

773

## 774 7. Author contribution

775

776 PK developed the initial concept for the study. All authors contributed with the collection of soil  
777 profiles at various sites. The PAGE21 incubation experiment was planned and conducted at  
778 CENPERM (University of Copenhagen) by SF, CJJ and BE, whereas the CryoCarb incubation  
779 experiments were carried out at the University of South Bohemia (Ceske Budejovice) under  
780 guidance of HS and JB. PK performed all statistical analyses, in cooperation with GH. All co-authors  
781 contributed to the writing of the manuscript, including its discussion section.

782

## 783 8. Competing interests

784

785 The authors declare that they have no conflict of interest.

786

## 787 9. Acknowledgments

788

789 Collection and laboratory analyses for Svalbard (Adventdalen and Ny Ålesund), Stordalen Mire and  
790 Lena Delta samples were supported by the EU-FP7 PAGE21 project (grant agreement no 282700).  
791 Lower Kolyma and Taymyr Peninsula samples were collected and incubated in the framework of the  
792 ESF-CryoCarb project, with support from the Swedish Research Council (VR to Kuhry), the  
793 Austrian Science Fund (FWF I370-B17 to Richter), the Czech Science Foundation (Project 16-  
794 18453S to Barta) and the Czech Soil-Water Research Infrastructure (MEYS CZ grants LM2015075  
795 and EF16-013/0001782 to Šantrůčková). Seida samples were originally collected in the framework  
796 of the EU-FP6 Carbo-North project (contract 036993). Gustaf Hugelius acknowledges a Swedish  
797 Research Council Marie Skłodowska Curie International Career Grant. Kateřina Diaková is  
798 acknowledged for the collection of the soil inoculi in Seida. The Seida samples were subsequently  
799 incubated at the University of South Bohemia. We are most grateful to Nikolai Lashchinskiy  
800 (Siberian Branch of the Russian Academy of Sciences, Novosibirsk) and Nikolaos Lampiris, Juri  
801 Palmtag, Nathalie Pluchon, Justine Ramage, Matthias Siewert and Martin Wik (all Stockholm  
802 University), for help in sample collection. We would also like to thank Magarethe Watzka  
803 (University of Vienna) for elemental analyses of soil samples. Zhanna Kuhrij is acknowledged for  
804 the preparation of Figures 5 and S6. We thank two anonymous reviewers for their constructive  
805 comments on the manuscript.

806

## 807 10. References

808

809 Bader, C., Müller, M., Schulin, R., and Leifeld, J.: Peat decomposability in managed organic soils in  
810 relation to land use, organic matter composition and temperature, *Biogeosciences* 15, 703-719,  
811 <https://doi.org/10.5194/bg-15-703-2018>, 2018.

- 812 Birch, H. F.: The effect of soil drying on humus decomposition and nitrogen availability, *Plant and*  
813 *Soil*, 10, 9-31, 1958.
- 814 Biskaborn, B. K., Smith, S. L., Noetzli, J., Matthes, H., Vieira, G., Streletskiy, D. A., Schoeneich, P.,  
815 Romanovsky, V. E., Lewkowicz, A. G., Abramov, A., Allard, M., Boike, J., Cable, W. L.,  
816 Christiansen, H. H., Delaloye, R., Diekmann, B., Drozdov, D., Eitzelmüller, B., Grosse, G.,  
817 Guglielmin, M., Ingeman-Nielsen, T., Isaksen, K., Ishikawa, M., Johansson, M., Johannsson, H.,  
818 Joo, A., Kaverin, D., Kholodov, A., Konstantinov, P., Kröger, T., Lambiel, C., Lanckman, J. P.,  
819 Luo, D., Malkova, G., Meiklejohn, I., Moskalenko, N., Oliva, M., Phillips, M., Ramos, M.,  
820 Sannel, A. B. K., Sergeev, D., Seybold, C., Skryabin, P., Vasiliev, A., Wu, Q., Yoshikawa, K.,  
821 Zheleznyak, M., and Lantuit, H.: Permafrost is warming at a global scale, *Nature*  
822 *Communications*, 10: 264, <https://doi.org/10.1038/s41467-018-08240-4>, 2019.
- 823 Bockheim, J. G.: Importance of cryoturbation in redistributing organic carbon in permafrost-affected  
824 soils, *Soil Sci. Soc. Am. J.* 71(4), 1335–1342, <https://doi.org/10.2136/sssaj2006.0414N>, 2007.
- 825 Brown, J., Ferrians Jr., O. J., Heginbottom, J. A., and Melnikov, E. S.: Circum-Arctic map of  
826 permafrost and ground-ice conditions, 1 : 10 000 000, Map CP-45, United States Geological  
827 Survey, International Permafrost Association, Washington, D. C., 1997.
- 828 Burke, E. J., Hartley, I. P., and Jones, C. D.: Uncertainties in the global temperature change caused  
829 by carbon release from permafrost thawing, *The Cryosphere*, 6, 1063–1076,  
830 <https://doi.org/10.5194/tc-6-1063-2012>, 2012.
- 831 Čapek, P., Diáková, K., Dickopp, J. E., Bárta, J., Wild, B., Schnecker, J., and Hugelius, G.: The  
832 effect of warming on the vulnerability of subducted organic carbon in arctic soils, *Soil Biol.*  
833 *Biochem.*, 90, 19-29, <https://doi.org/10.1016/j.soilbio.2015.07.013>, 2015.
- 834 Ciais, P.: A geoscientist is astounded by Earth’s huge frozen carbon deposits, *Nature*, 462, 393,  
835 <https://doi.org/10.1038/462393e>, 2009.
- 836 Clymo, R. S. and Hayward, P. M.: The Ecology of *Sphagnum*, in: Smith, A. J. E. (ed). *Bryophyte*  
837 *Ecology*. 540, 229–289, [https://doi.org/10.1007/978-94-009-5891-3\\_8](https://doi.org/10.1007/978-94-009-5891-3_8), 1982.
- 838 Davidson, E. A. and Janssens, I. A.: Temperature sensitivity of soil carbon decomposition and  
839 feedbacks to climate change, *Nature*, 440, 165–173, <https://doi.org/10.1038/nature04514>, 2006.
- 840 Diáková, K., Čapek, P., Kohoutová, I., Mpamah, P., Barta, J., Biasi, C., Martikainen, P., and  
841 Šantrůčková, H.: Heterogeneity of carbon loss and its temperature sensitivity in East-European  
842 subarctic tundra soils, *FEMS Microbiol. Ecol.*, 92: fiw140,  
843 <https://doi.org/10.1093/femsec/fiw140>, 2016.
- 844 Elberling, B., Michelsen, A., Schädel, C., Schuur, E. A., Christiansen, H. H., Berg, L., Tamstorf, M.  
845 P., and Sigsgaard, C.: Long-term CO<sub>2</sub> production following permafrost thaw, *Nature Climate*  
846 *Change*, 3(10), 890–894, <https://doi.org/10.1038/nclimate1955>, 2013.
- 847 Faucherre, S., Jørgensen, C. J., Blok, D., Weiss, N., Siewert, M. B., Bang-Andreasen, T., Hugelius,  
848 G., Kuhry, P., and Elberling, B.: Short and long-term controls on active layer and permafrost  
849 carbon turnover across the Arctic, *J. Geophys. Res.--Biogeosciences.*, 123(2), 372–390.,  
850 <https://doi.org/10.1002/2017JG004069>, 2018.
- 851 Fierer, N. and Schimel, J. P.: A proposed mechanism for the pulse in carbon dioxide production  
852 commonly observed following the rapid rewetting of a dry soil. *Soil Sci. Soc. Am. J.*, 67(3),  
853 798–805, <https://doi.org/10.2136/sssaj2003.0798>, 2003.
- 854 Franzluebbers, A. J., Haney, R. L., Honeycutt, C. W., Schomberg, H. H., and Hons, F. M.: Flush of  
855 carbon dioxide following rewetting of dried soil relates to active organic pools, *Soil Sci. Soc.*  
856 *Am. J.*, 64(2), 613–623, <https://doi.org/10.2136/sssaj2000.642613x>, 2000.
- 857 Gentsch, N., Mikutta, R., Alves, R. J. E., Barta, J., Čapek, P., Gittel, A., Hugelius, G., Kuhry, P.,  
858 Lashchinskiy, N., Palmtag, J., Richter, A., Šantrůčková, H., Schnecker, J., Shibistova, O., Urich,

859 T., Wild, B., and Guggenberger, G.: Storage and transformation of organic matter fractions in  
860 cryoturbated permafrost soils across the Siberian Arctic, *Biogeosciences*, 12(14): 4525–4542,  
861 <https://doi.org/10.5194/bg-12-4525-2015>, 2015a.

862 Gentsch, N., Mikutta, R., Shibistova, O., Wild, B., Schnecker, J., Richter, A., and Guggenberger, G.:  
863 Properties and bioavailability of particulate and mineral-associated organic matter in Arctic  
864 permafrost soils, Lower Kolyma Region, Russia. *European J. Soil Sci.*, 66: 722–734,  
865 <https://doi.org/10.1111/ejss.12269>, 2015b.

866 Gentsch, N., Wild, B., Mikutta, R., Čapek, P., Diáková, K., Schrumppf, M., Turner, S., Minnich, C.,  
867 Schaarschmidt, F., Shibistova, O., Schnecker, J., Urich, T. Gittel, A., Šantrůčková, H., Bárta, J.,  
868 Lashchinskiy, N., Fuß, R., Richter, A., and Guggenberger, G.: Temperature response of  
869 permafrost soil carbon is attenuated by mineral protection. *Glob. Change Biol.*, 24: 3401–3415,  
870 <https://doi.org/10.1111/gcb.14316>, 2018.

871 Gittel, A., Bárta, J., Kohoutová, I., Mikutta, R., Owens, S., Gilbert, J., Schnecker, J., Wild, B.,  
872 Hannisdal, B., Maerz, J., Lashchinskiy, N., Čapek, P., Šantrůčková, H., Gentsch, N., Shibistova,  
873 O., Guggenberger, G., Richter, A., Torsvik, V. L., Schleper, C., and Urich, T.: Distinct microbial  
874 communities associated with buried soils in the Siberian tundra, *ISME J.*, 8, 841–853, 2014.

875 Grosse, G., Harden, J., Turetsky, M. R., McGuire, A. D., Camill, P., Tarnocai, C., Frolking, S.,  
876 Schuur, E. A. G., Jorgenson, T., Marchenko, S., Romanovsky, V., Wickland, K. P., French, N.,  
877 Waldrop, M. P., Bourgeau-Chavez, L., and Striegl, R. G.: Vulnerability of high-latitude soil  
878 organic carbon in North America to disturbance, *J. Geophys. Res.*, 116, G00K06,  
879 <https://doi.org/10.1029/2010JG001507>, 2011.

880 Grosse, G., Robinson, J. E., Bryant, R., Taylor, M. D., Harper, W., DeMasi, A., Kyker-Snowman, E.,  
881 Veremeeva, A., Schirrmeister, L., and Harden, J.: Distribution of late Pleistocene ice-rich  
882 syngenetic permafrost of the Yedoma suite in east and central Siberia, Russia, U. S. Geological  
883 Survey Open File Report, 1078, 37 pp., 2013.

884 Gruber, N., Friedlingstein, P., Field, C. B., Valentini, R., Heimann, M., Richey, J. E., Romero-  
885 Lankao, P., Schulze, D., and Chen, C.-T. A.: The vulnerability of the carbon cycle in the 21<sup>st</sup>  
886 century: An assessment of carbon-climate-human interactions, in: *The Global Carbon Cycle,*  
887 *Integrating Humans, Climate and the Natural World*, edited by: Field, C. and Raupach, M.,  
888 Island Press, Washington D. C., 45–76, 2004.

889 Hammer, Ø., Harper, D.A.T., and Ryan, P. D.: PAST: Paleontological Statistics Software Package  
890 for Education and Data Analysis. *Palaeontologia Electronica*, 4(1), 9 pp., 178kb, [http://palaeo-](http://palaeo-electronica.org/2001_1/past/issue1_01.htm)  
891 [electronica.org/2001\\_1/past/issue1\\_01.htm](http://palaeo-electronica.org/2001_1/past/issue1_01.htm), 2001.

892 Harden, J. W., Koven, C. D., Ping, C. L., Hugelius, G., McGuire, A. D., Camill, P., Jorgenson, T.,  
893 Kuhry, P., Michaelson, G. J., O'Donnell, J. A., Schuur, E. A. G., Tarnocai, C., Johnson, K., and  
894 Grosse, G.: Field information links permafrost carbon to physical vulnerabilities of thawing,  
895 *Geophys. Res. Lett.*, 39, L15704 <https://doi.org/10.1029/2012gl051958>, 2012.

896 Horwath Burnham, J. and Sletten, R. S.: Spatial distribution of soil organic carbon in northwest  
897 Greenland and underestimates of High Arctic carbon stores, *Global Biogeochem. Cy.*, 24,  
898 GB3012, <https://doi.org/10.1029/2009GB003660>, 2010.

899 Hugelius, G. and Kuhry, P.: Landscape partitioning and environmental gradient analyses of soil  
900 organic carbon in a permafrost environment, *Global Biogeochem. Cy.*, 23, GB3006,  
901 <https://doi.org/10.1029/2008GB003419>, 2009.

902 Hugelius, G., Kuhry, P., Tarnocai, C., and Virtanen, T.: Soil organic carbon pools in a periglacial  
903 landscape: a case study from the central Canadian Arctic, *Permafrost Periglac.*, 21, 16–29,  
904 <https://doi.org/10.1002/ppp.677>, 2010.

905 Hugelius, G., Virtanen, T., Kaverin, D., Pastukhov, A., Rivkin, F., Marchenko, S., Romanovsky, V.,  
906 and Kuhry, P.: High-resolution mapping of ecosystem carbon storage and potential effects of  
907 permafrost thaw in periglacial terrain, European Russian Arctic, *J. Geophys. Res.*, 116, G03024,  
908 <https://doi.org/10.1029/2010JG001606>, 2011.

909 Hugelius, G., Strauss, J., Zubrzycki, S., Harden, J. W., Schuur, E. A. G., Ping, C.-L., Schirrmeister,  
910 L., Grosse, G., Michaelson, G. J., Koven, C. D., O'Donnell, J. A., Elberling, B., Mishra, U.,  
911 Camill, P., Yu, Z., Palmtag, J., and Kuhry, P.: Estimated stocks of circumpolar permafrost  
912 carbon with quantified uncertainty ranges and identified data gaps, *Biogeosciences*, 11, 6573–  
913 6593, <https://doi.org/10.5194/bg-11-6573-2014>, 2014.

914 Hugelius, G., Kuhry, P., and Tarnocai, C.: Ideas and perspectives: Holocene thermokarst sediments  
915 of the Yedoma permafrost region do not increase the northern peatland carbon pool.  
916 *Biogeosciences*, 13, 2003–2010, <https://doi.org/10.5194/bg-13-2003-2016>, 2016.

917 IPCC: Summary for Policymakers, in: *Climate Change 2013: The Physical Science Basis.*  
918 *Contribution of Working Group I to the Fifth Assessment Report of the Intergovernmental Panel*  
919 *on Climate Change*, edited by: Stocker, T. F., Qin, D., Plattner, G.-K., Tignor, M., Allen, S. K.,  
920 Boschung, J., Nauels, A., Xia, Y., Bex, V., and Midgley, P. M., Cambridge University Press,  
921 Cambridge, United Kingdom and New York, NY, USA, 2013.

922 IPCC: Summary for Policymakers, in: *Global Warming of 1.5 °C. An IPCC Special Report on the*  
923 *impacts of global warming of 1.5°C above pre-industrial levels and related global greenhouse*  
924 *gas emission pathways, in the context of strengthening the global response to the threat of*  
925 *climate change, sustainable development, and efforts to eradicate poverty*, edited by Masson-  
926 Delmotte, V., Zhai, P., Pörtner, H.-O., Roberts, D., Skea, J., Shukla, P. R., Pirani, A.,  
927 Moufouma-Okia, W., Péan, C., Pidcock, R., Connors, S., Matthews, J. B. R., Chen, Y., Zhou,  
928 X., Gomis, M. I., Lonnoy, E., Maycock, T., Tignor, M., and Waterfield, T., World  
929 Meteorological Organization, Geneva, Switzerland, 32 pp., 2018. Jarvis, P., Rey, A., Petsikos,  
930 C., Wingate, L., Rayment, M., Pereira, J., Banza, J., David, J., Miglietta, F., Borghetti, M.,  
931 Manca, G. and Valentini, R.: Drying and wetting of Mediterranean soils stimulates  
932 decomposition and carbon dioxide emission: the “Birch effect”, *Tree Physiology*, 27: 929–940,  
933 2007.

934 Kaiser, C., Meyer, H., Biasi, C., Rusalimova, O., Barsukov, P., and Richter, A.: Conservation of soil  
935 organic matter through cryoturbation in arctic soils in Siberia, *J. Geophys. Res.*, 112, G02017,  
936 <https://doi.org/10.1029/2006JG000258>, 2007.

937 Knoblauch, C., Beer, C., Sosnin, A., Wagner, D. and Pfeiffer, E.-M.: Predicting long-term carbon  
938 mineralization and trace gas production from thawing permafrost of Northeast Siberia, *Glob.*  
939 *Change Biol.*, 19, 1160–1172, <https://doi.org/10.1111/gcb.12116>, 2013.

940 Kuhry, P.: The role of fire in the development of *Sphagnum*-dominated peatlands in Western Boreal  
941 Canada, *J. Ecol.*, 82(4): 899-910, <http://www.jstor.org/stable/2261453>, 1994.

942 Kuhry, P. and Vitt, D. H.: Fossil carbon/nitrogen ratios as a measure of peat decomposition, *Ecology*,  
943 77, 271–275, <https://doi.org/10.2307/2265676>, 1996.

944 Kuhry, P., Dorrepaal, E., Hugelius, G., Schuur, E. A. G., and Tarnocai, C.: Potential remobilization  
945 of belowground permafrost carbon under future global warming, *Permafrost Periglac.*, 21, 208–  
946 214, <https://doi.org/10.1002/ppp.684>, 2010.

947 NCSCDv2: Doi:10.5879/ECDS/00000002, 2014.

948 Olefeldt, D., Turetsky, M. R., Crill, P. M., and McGuire, A. D.: Environmental and physical controls  
949 on northern terrestrial CH<sub>4</sub> emissions across permafrost zones, *Glob. Change Biol.*, 19, 589–  
950 603, <https://doi.org/10.1111/gcb.12071>, 2013.

- 951 Palmtag, J., Hugelius, G., Lashchinskiy, N., Tamstorf, M. P., Richter, A., Elberling, B., and Kuhry,  
 952 P.: Storage, landscape distribution and burial history of soil organic matter in contrasting areas  
 953 of continuous permafrost, *Arct. Antarct. Alp. Res.*, 47, 71–88,  
 954 <https://doi.org/10.1657/AAAR0014-027>, 2015.
- 955 Palmtag, J., Ramage, J., Hugelius, G., Gentsch, N., Lashchinskiy, N., Richter, A., and Kuhry, P.:  
 956 Controls on the storage of organic carbon in permafrost soils in northern Siberia, *Eur. J. Soil*  
 957 *Sci.*, 67, 478–491, <https://doi.org/10.1111/ejss.12357>, 2016.
- 958 Palmtag, J. and Kuhry, P.: Grain size controls on cryoturbation and soil organic carbon density in  
 959 permafrost-affected soils, *Permafrost Periglac.*, 29, 112–120, <https://doi.org/10.1002/ppp.1975>,  
 960 2018.
- 961 Ping, C.-L., Michaelson, G. J., Jorgenson, M. T., Kimble, J. M., Epstein, H., Romanovsky, V. E., and  
 962 Walker, D. A.: High stocks of soil organic carbon in North American Arctic region, *Nat.*  
 963 *Geosci.*, 1, 615–619, <https://doi.org/10.1038/ngeo284>, 2008.
- 964 Šantrůčková, H., Kurbatova, J., Shibistova, O., Smejkalova, M., and Kastovska, E.: Short-Term  
 965 Kinetics of Soil Microbial Respiration – A General Parameter Across Scales ? In: *Tree Species*  
 966 *Effects on Soils: Implications for Global Change*, Proceedings of the NATO Advanced Research  
 967 Workshop on Trees and Soil Interactions, Implications to Global Climate Change, August 2004,  
 968 Krasnoyarsk, Russia, pp. 229-246, [https://doi.org/10.1007/1-4020-3447-4\\_13](https://doi.org/10.1007/1-4020-3447-4_13), 2006.
- 969 Schuur, E. A. G., Bockheim, J., Canadell, J. G., Euskirchen, E., Field, C. B., Goryachkin, S. V.,  
 970 Hagemann, S., Kuhry, P., Laflour, P. M., Lee, H., Mazhitova, G., Nelson, F. E., Rinke, A.,  
 971 Romanovsky, V. E., Shiklomanov, N., Tarnocai, C., Venevsky, S., Vogel, J. G., and Zimov, S.  
 972 A.: Vulnerability of Permafrost Carbon to Climate Change: Implications for the Global Carbon  
 973 Cycle, *Bioscience*, 58(8), 701–714, <https://doi.org/10.1641/B580807>, 2008.
- 974 Schuur, E. A. G., McGuire, A. D., Schädel, C., Grosse, G., Harden, J. W., Hayes D. J., Hugelius, G.,  
 975 Koven, C. D., Kuhry, P., Lawrence, D. M., Natali, S. M., Olefeldt, D., Romanovsky, V. E.,  
 976 Schaefer, K., Turetsky, M. R., Treat, C. C., and Vonk, J. E.: Climate change and the permafrost  
 977 carbon feedback, *Nature*, 20, 171–179, <https://doi.org/10.1038/nature14338>, 2015.
- 978 Schädel, C., Schuur, E. A. G., Bracho, R., Elberling, B., Knoblauch, C., Lee, H., Luo, Y., Shaver, G.  
 979 R., and Turetsky, M. R.: Circumpolar assessment of permafrost C quality and its vulnerability  
 980 over time using long-term incubation data, *Glob. Change Biol.*, 20, 641–652,  
 981 <https://doi.org/10.1111/gcb.12417>, 2014.
- 982 Shmelev, D., Veremeeva, A., Kraev, G., Kholodov, A., Spencer, R. G. M., and Walker, W. S.:  
 983 Estimation and Sensitivity of Carbon Storage in Permafrost of North-Eastern Yakutia,  
 984 *Permafrost. Periglac.*, 28, 379–390, <https://doi.org/10.1002/ppp.1933>, 2017.
- 985 Siewert, M. B., Hugelius, G., Heim, B., and Faucherre, S.: Landscape controls and vertical  
 986 variability of soil organic carbon storage in permafrost-affected soils of the Lena River Delta,  
 987 *CATENA*, 147, 725–741, <https://doi.org/10.1016/j.catena.2016.07.048>, 2016.
- 988 Siewert, M. B.: High-resolution digital mapping of soil organic carbon in permafrost terrain using  
 989 machine learning: a case study in a sub-Arctic peatland environment, *Biogeosciences*, 15, 1663–  
 990 1682, <https://doi.org/10.5194/bg-15-1663-2018>, 2018.
- 991 Schneckner, J., Wild, B., Hofhansl, F., Eloy Alves, R. J., Bárta, J., Čapek, P., Fuchslueger, L.,  
 992 Gentsch, N., Gittel, A., Guggenberger, G., Hofer, A., Kienzl, S., Knoltsch, A., Lashchinskiy, N.,  
 993 Mikutta, R., Šantrůčková, H., Shibistova, O., Takriti, M., Ulrich, T., Weltin, G., and Richter, A.:  
 994 Effects of soil organic matter properties and microbial community composition on enzyme  
 995 activities in cryoturbated arctic soils, *PLoS ONE*, 9, e94076,  
 996 <https://doi.org/10.1371/journal.pone.0094076>, 2014.

- 997 Soil Survey Staff: Keys to Soil Taxonomy, Twelfth Edition, USDA Natural Resources Conservation  
998 Service, Washington, D.C., 2014.
- 999 Strauss, J., Schirrmeyer, L., Grosse, G., Wetterich, S., Ulrich, M., Herzsich, U., and Hubberten,  
1000 H.-W.: The deep permafrost carbon pool of the Yedoma region in Siberia and Alaska, *Geophys.*  
1001 *Res. Lett.*, 40, 6165–6170, <https://doi.org/10.1002/2013GL058088>, 2013.
- 1002 Tarnocai, C., Canadell, J. G., Schuur, E. A. G., Kuhry, P., Mazhitova, G., and Zimov, S.: Soil  
1003 organic carbon pools in the northern circumpolar permafrost region, *Global Biogeochem. Cy.*,  
1004 23, GB2023, <https://doi.org/10.1029/2008GB003327>, 2009.
- 1005 Vardy, S. R., Warner, B. G., Turunen, J., and Aravena, R.: Carbon accumulation in permafrost  
1006 peatlands in the Northwest Territories and Nunavut, Canada, *Holocene*, 10, 273–280,  
1007 <https://doi.org/10.1191/095968300671749538>, 2000.
- 1008 Walter Anthony, K. M., Zimov, S. A., Grosse, G., Jones, M. C., Anthony, P. M., Iii, F. S. C., Finlay,  
1009 J. C., Mack, M. C., Davydov, S., Frenzel, P., and Frolking, S.: A shift of thermokarst lakes from  
1010 carbon sources to sinks during the Holocene epoch, *Nature*, 511, 452–456,  
1011 <https://doi.org/10.1038/nature13560>, 2014.
- 1012 Weiss, N., Blok, D., Elberling, B., Hugelius, G., Jorgensen, C. J., Siewert, M. B., and Kuhry, P.:  
1013 Thermokarst dynamics and soil organic matter characteristics controlling initial carbon release  
1014 from permafrost soils in the Siberian Yedoma region, *Sediment. Geol.*, 340, 38–48,  
1015 <https://doi.org/10.1016/j.sedgeo.2015.12.004>, 2016.
- 1016 Weiss, N., Faucherre, S., Lampiris, N., and Wojcik, R.: Elevation-based upscaling of organic carbon  
1017 stocks in high Arctic permafrost terrain: A storage and distribution assessment for Spitsbergen,  
1018 Svalbard, *Polar Research*, 36(1), <https://doi.org/10.1080/17518369.2017.1400363>, 2017.
- 1019 Weiss, N. and Kaal, J.: Characterization of labile organic matter in Pleistocene permafrost (NE  
1020 Siberia), using Thermally assisted Hydrolysis and Methylation (THM-GC-MS), *Soil Biol.*  
1021 *Biochem.*, 117, 203–213, <https://doi.org/10.1016/j.soilbio.2017.10.001>, 2018.
- 1022 Zechmeister-Boltenstern, S., Keiblinger, K. M., Mooshammer, M., Penuelas, J., Richter, A., Sardans,  
1023 J., and Wanek, W.: The application of ecological stoichiometry to plant–microbial–soil organic  
1024 matter transformations, *Ecol. Monographs*, 85, 133–155, <https://doi.org/10.1890/14-0777.1>,  
1025 2015.

1026  
1027

1028

1029 Tables

1030

1031 Pages 23-26

1032

1033

1034

1035 Figures

1036

1037 Pages 27-31

1038

Table 1

	%C vs C/N	%C vs DBD	C/N vs DBD
Correlation	positive	negative	negative
PAGE21, All sites	0.53 (228)	0.67 (232)	0.57 (228)
CryoCarb 1-Kolyma	0.79 (418)	0.78 (413)	0.63 (413)
CryoCarb 2-Taymyr	0.64 (484)	0.69 (480)	0.47 (480)
CryoCarb 3-Seida	0.47 (71)	0.84 (79)	0.47 (71)

Table 2

	DBD vs C release/gdw	%C vs C release/gdw	C/N vs C release/gdw
Correlation	negative	positive	positive
PAGE21, All sites	0.52 (232)	0.45 (232)	0.34 (228)
CryoCarb 1-Kolyma	0.52 (404)	0.47 (406)	0.54 (406)
CryoCarb 2-Taymyr	0.41 (480)	0.33 (484)	0.48 (484)
CryoCarb 3-Seida	0.81 (78)	0.43 (78)	0.38 (70)

Table 3

a

	Pt	Min/CE	Min Mtn	Min Pty	Min Lowl	Alluv	Eol	PI Yed
PAGE21, All sites	0.24	0.29	0.99	1.51	1.44	1.44	1.68	
CryoCarb-Kolyma	4.83	6.72	17.8	15.3	19.7	22.0		11.5
CryoCarb-Taymyr	6.24			29.3	24.7	26.2		
CryoCarb-Seida	2,40			5.76	7.92			

b

	Pt	Min/CE	Min Mtn	Min Pty	Min Lowl	Alluv	Eol	PI Yed
PAGE21, All sites	0.17	0.20	0.69	1.05	1	1.00	1.17	
CryoCarb-Kolyma	0.25	0.34	0.90	0.78	1	1.12		0.58
CryoCarb-Taymyr	0.26			1.18	1	1.06		
CryoCarb-Seida	0.30			0.73	1			
Mean relative lability	0.24	0.27	0.80	0.94	1	1.06	1.17	0.58
S.D. relative lability	0.05	0.10	0.15	0.22		0.06		

Table 4

a

	AL_Min	AL_Ce	P_Min	P_Ce	AL_Pt	OL Ls	Min Ls	Min Ls	
AL_OL	< 0.001	0.0072	< 0.001	< 0.001	< 0.001	0.0493	< 0.001	< 0.001	AL_OL
AL_Min		0.5761	0.2217	0.5360	0.1887	< 0.001	0.6598	0.5682	AL_Min
AL_Ce			0.1464	0.1387	0.5186	0.0160	0.1956	0.7096	AL_Ce
P_Min				0.5570	0.0119	< 0.001	0.7353	0.0809	P_Min
P_Ce					0.0119	< 0.001	1.0000	0.1828	P_Ce
AL_Pt						0.0018	0.0518	0.1103	AL_Pt
AL_OL Ls							< 0.001	< 0.001	AL_OL Ls
AL_Min Ls								0.2500	AL_Min Ls

b

	AL_Min	AL_Ce	P_Min	P_Ce	AL_Pty	AL_Pt	P_Pt	Fr_Yed	Th_Yed	
AL_OL	0.3800	0.0027	0.0658	< 0.001	0.0255	< 0.001	< 0.001	< 0.001	< 0.001	AL_OL
AL_Min		< 0.001	0.011	< 0.001	0.0174	< 0.001	< 0.001	< 0.001	< 0.001	AL_Min
AL_Ce			0.1178	0.2318	0.8849	0.0083	< 0.001	0.3428	0.1653	AL_Ce
P_Min				< 0.001	0.1656	< 0.001	< 0.001	0.0017	< 0.001	P_Min
P_Ce					0.4539	0.0098	< 0.001	0.9258	0.2751	P_Ce
AL_Pty						0.0168	< 0.001	0.5059	0.2036	AL_Pty
AL_Pt							0.0440	< 0.001	0.0034	AL_Pt
P_Pt								< 0.001	< 0.001	P_Pt
Fr_Yed									0.1448	Fr_Yed

Figure 1

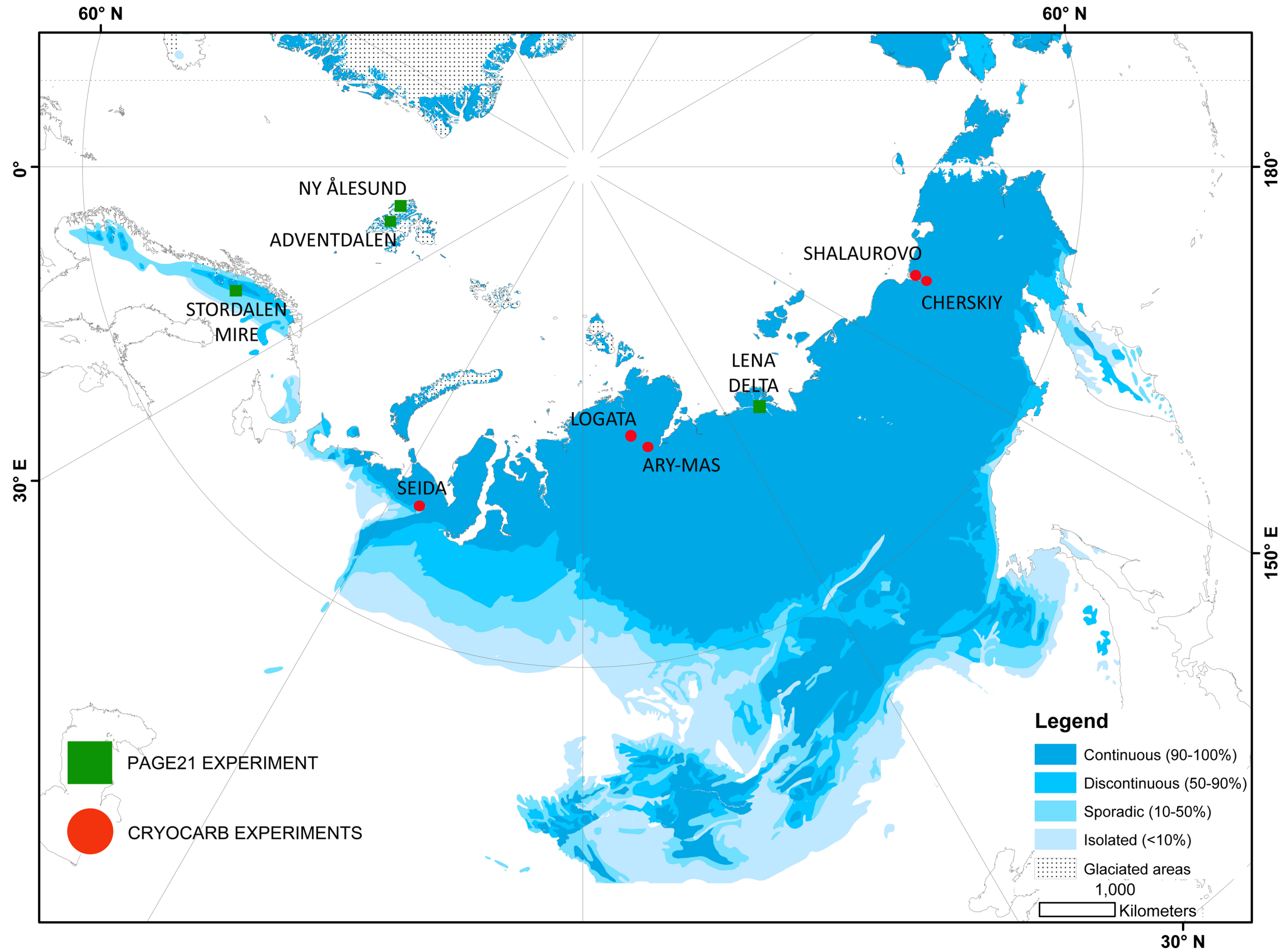
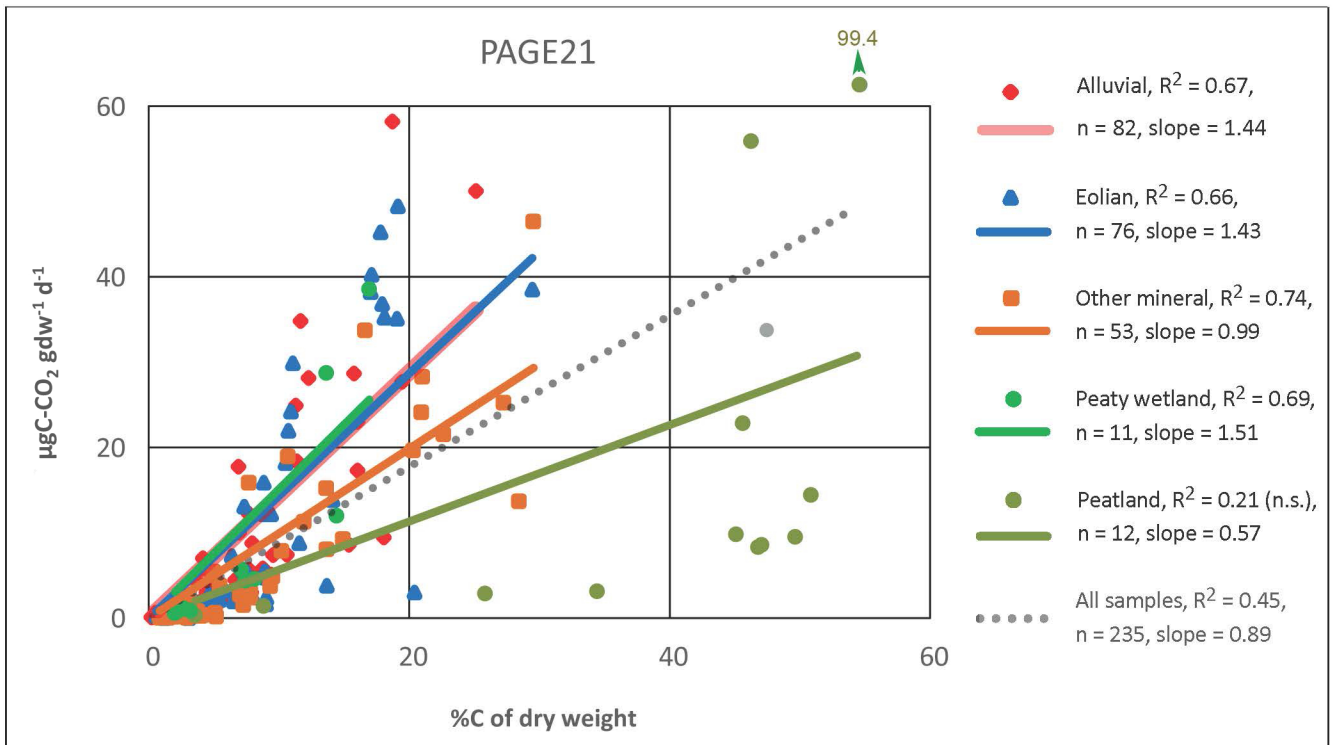


Figure 2

a



b

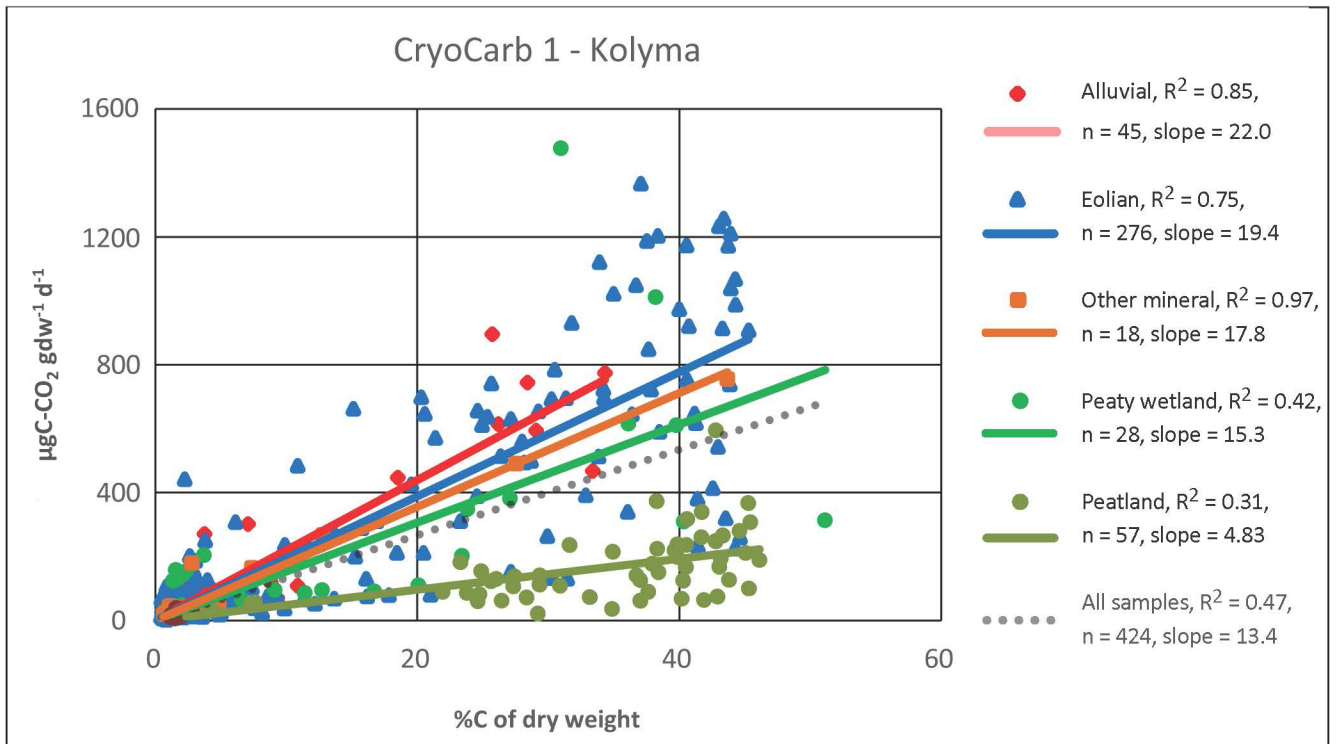
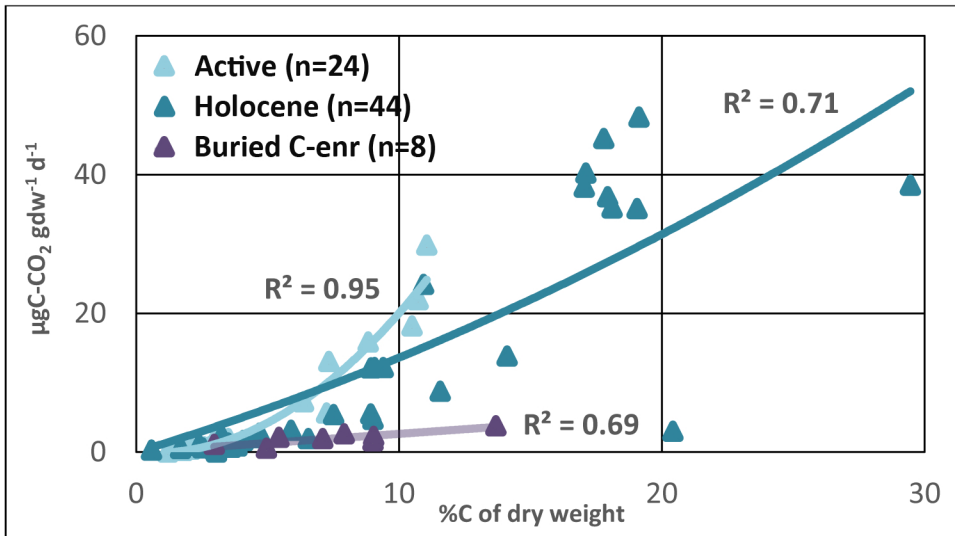
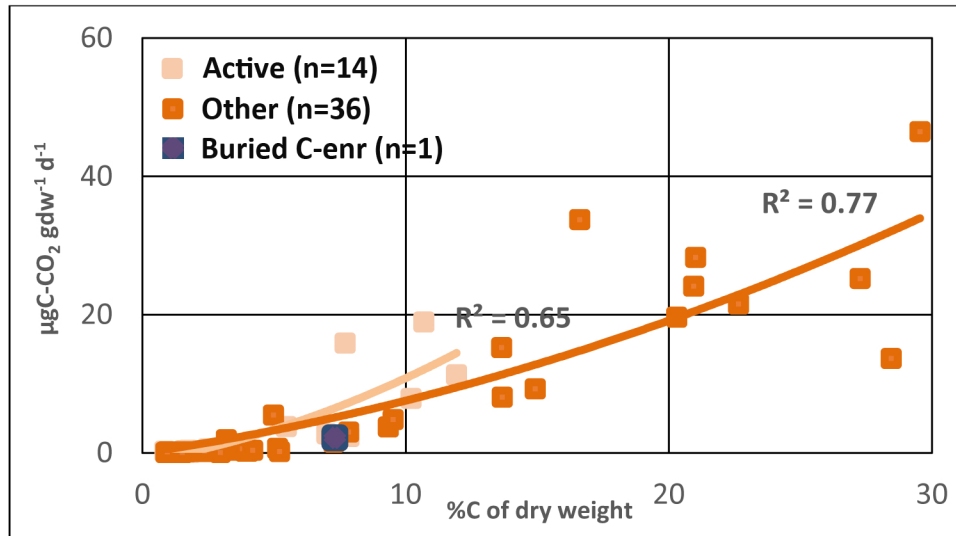


Figure 3

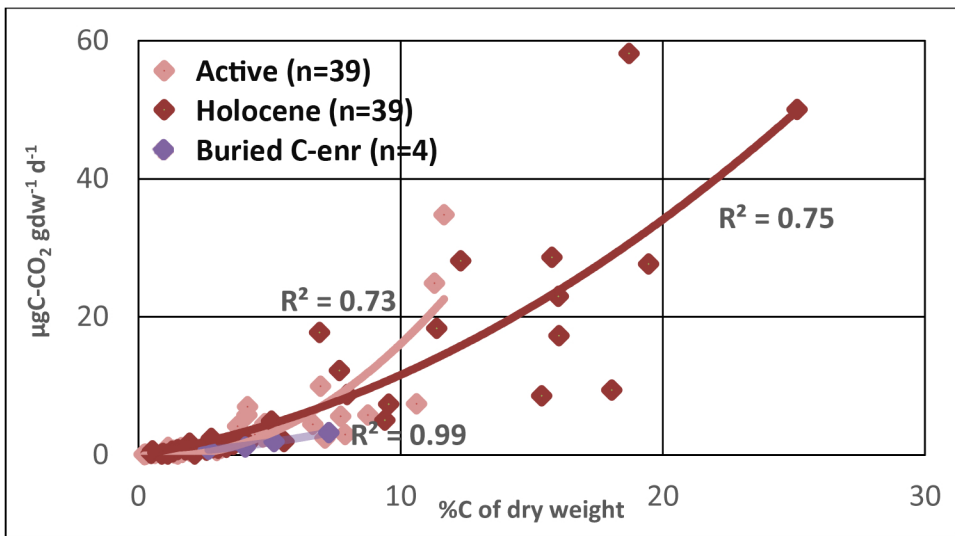
a. Eolian (n=76)



c. Mineral (n=51)



b. Alluvial (n=82)



d. Wetland (n=24)

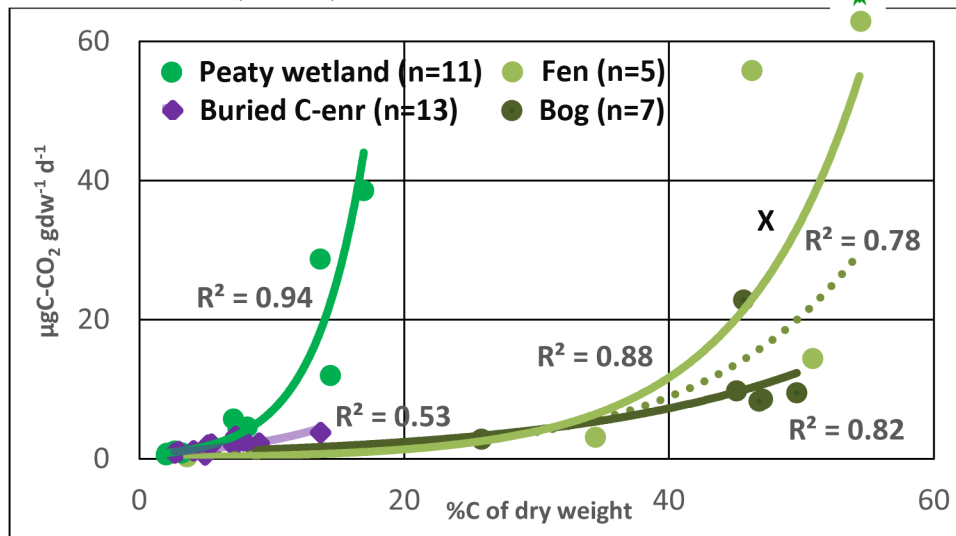
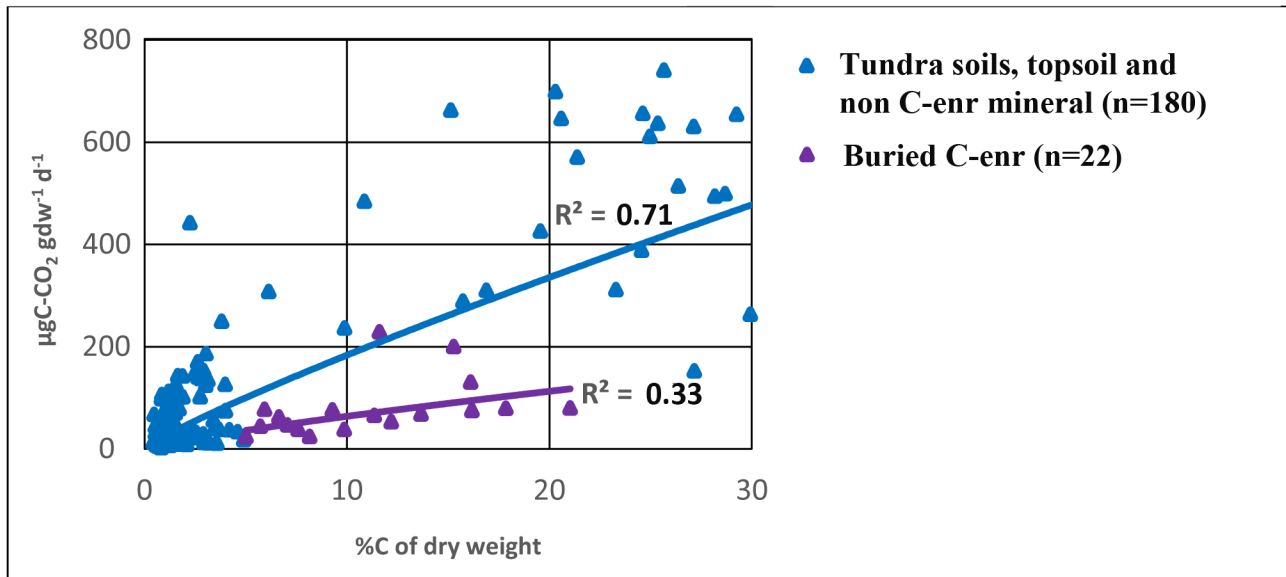


Figure 4

a



b

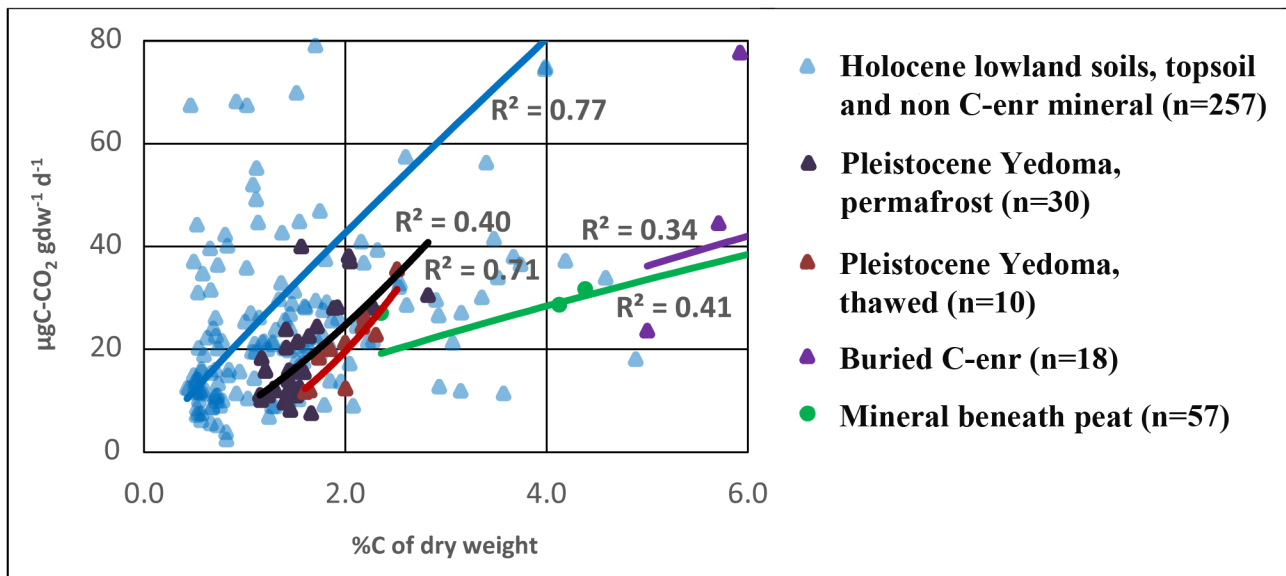
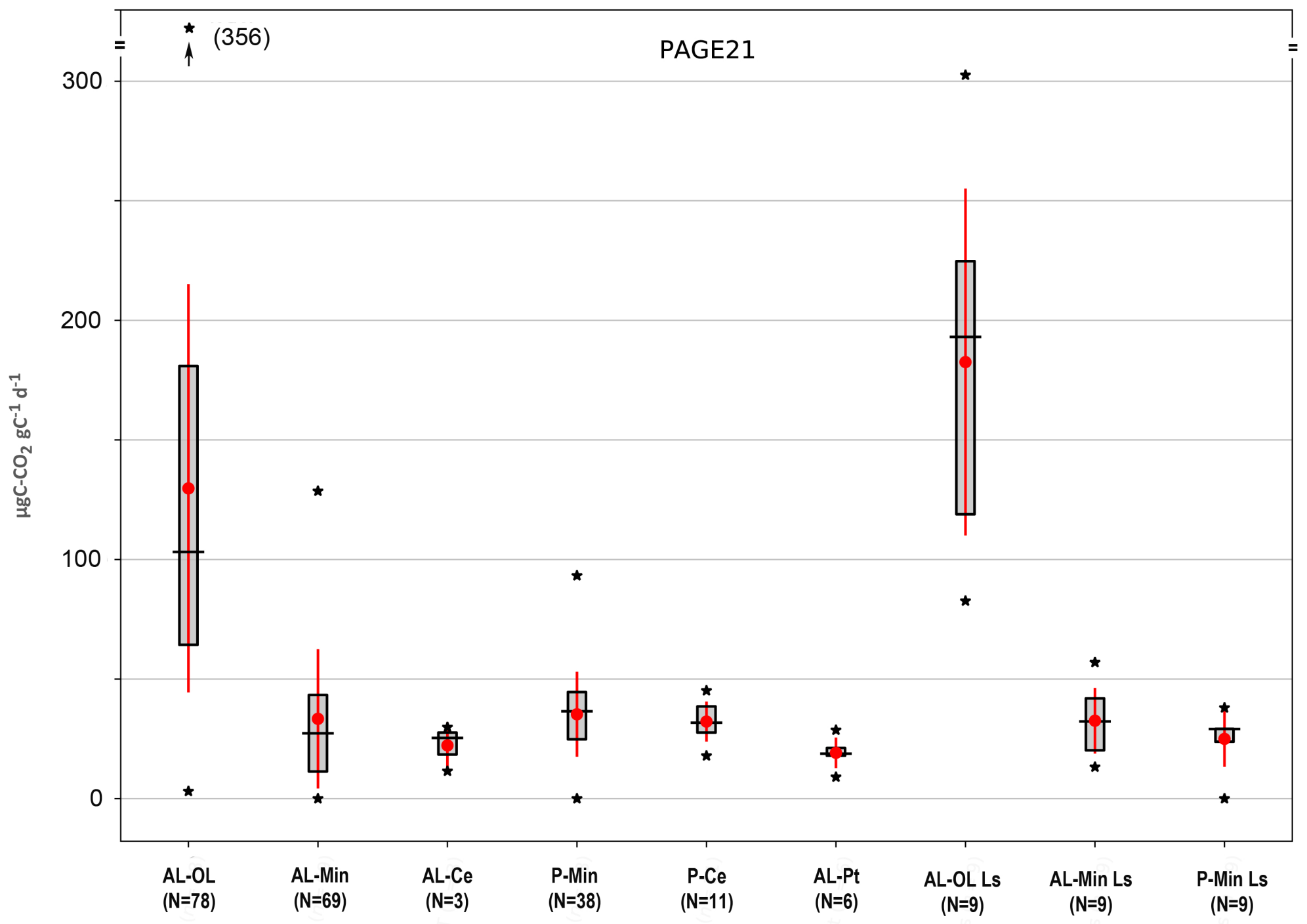


Figure 5

a



b

